General tests for $t\to W^+b$ couplings at hadron colliders

Charles A. Nelson,* Brian T. Kress, Marco Lopes, and Thomas P. McCauley
Department of Physics, State University of New York at Binghamton, Binghamton, New York 13902-6016
(Received 23 June 1997)

The modularity property of the helicity formalism is used to provide amplitude expressions and stage-two spin-correlation functions which can easily be used in direct experimental searches for electroweak symmetries and dynamics in the decay processes $t\to W^+b$ and $\overline{t}\to W^-\overline{b}$. The formalism is used to describe the decay sequences $t\to W^+b\to(l^+\nu)b$ and $t\to W^+b\to(j_{\overline{d}}j_u)b$. Helicity amplitudes for $t\to W^+b$ are obtained for the most general $J_{\overline{bt}}$ current. Thereby, the most general Lorentz-invariant decay density matrix for $t\to W^+b\to(l^+\nu)b$ or for $t\to W^+b\to(j_{\overline{d}}j_u)b$ is expressed in terms of eight helicity parameters and, equivalently, in terms of the structures of the $J_{\overline{bt}}$ current. The parameters are physically defined in terms of partial-width intensities for polarized final states in $t\to W^+b$ decay. The full angular distribution for the reactions $q\overline{q}$ and $gg\to t\overline{t}\to(W^+b)(W^-\overline{b})\to\cdots$ can be used to measure these parameters. Since this adds on spin-correlation information from the next stage of decays in the decay sequence, such an energy-angular distribution is called a stage-two spin-correlation function. [S0556-2821(97)03321-3]

PACS number(s): 14.65.Ha, 11.30.Er, 11.30.Qc

I. INTRODUCTION

While in the standard model violations of CP, T, and $(V-A)$ symmetry are phenomenologically well described by the Higgs mechanism and the Cabibbo-Kobayashi-Maskawa (CKM) matrix, the depth of the dynamical understanding remains open to question. In particular, the Yukawa couplings of the fermions and the CKM mixing angles and CP phase parameter are inserted by hand. For this reason and the new fermionic mass scale of ~ 175 GeV provided by the recently discovered top quark [1–3], it is important to probe for new and/or additional symmetry violations at $m_t \sim 175$ GeV.

We use the modularity property of the helicity formalism [4] to provide amplitude expressions and stage-two spin-correlation functions which can easily be used in direct experimental searches for electroweak symmetries and dynamics in the decay processes $t\to W^+b$ and $\overline{t}\to W^-\overline{b}$. Stage-two spin-correlation functions are also a useful technique for testing the symmetry properties and dynamics of $t\overline{t}$ pair production in both the $q\overline{q}\to t\overline{t}$ and $gg\to t\overline{t}$ channels [5,6].

The reader should be aware that it is not necessary to use the helicity formalism [4] because the observables are physically defined in terms $t\to W^+b$ decay partial-width intensities for polarized final states. However, the helicity formalism does provide a lucid, flexible, physical framework for connecting Lorentz-invariant couplings at the Lagrangian level with Lorentz-invariant spin-correlation functions. In practice, the helicity formalism also frequently provides insights and easy checks on the resulting formulas.

The literature on polarimetry methods and spin-correlation functions in t quark physics includes Refs. [5,7,6]. Literature on methods to test for CP violation in t reactions include Refs. [5,8,9,6].

In this paper, we concentrate on the most general Lorentz-invariant decay density matrix $R_{\lambda_1,\lambda_1'}$ for $t\to W^+b\to(l^+\nu)b$ or for $t\to W^+b\to(j_{\overline{d}}j_u)b$, where $\lambda_1,\lambda_1'=\pm 1/2$ is the t helicity. $R_{\lambda_1,\lambda_1'}$ is expressed in terms of eight helicity parameters [6,10]. The diagonal elements are simply the angular distributions $dN/d(\cos\theta_1^t)d(\cos\widetilde{\theta}_a)d\widetilde{\phi}_a$ for the polarized t decay chain, $t\to W^+b\to(l^+\nu)b$ or $t\to W^+b\to(j_{\overline{d}}j_u b)$.

There are eight $t\to W^+b$ decay parameters since there are the four $W_{L,T}b_{L,R}$ final-state combinations: The first parameter is simply $\Gamma\equiv\Gamma_L^+ + \Gamma_T^+$, i.e., the partial width for $t\to W^+b$. The subscripts on the Γ's denote the polarization of the final W^+, either $L=$''longitudinal'' or $T=$''transverse''; superscripts denote ''$\pm$ for sum or difference of the b_L versus b_R contributions.'' In terms of the helicity amplitudes defined in Sec. II,

$$\Gamma_L^{\pm}=|A(0,-\tfrac{1}{2})|^2\pm|A(0,\tfrac{1}{2})|^2,$$

$$\Gamma_T^{\pm}=|A(-1,-\tfrac{1}{2}|)^2\pm|A(1,\tfrac{1}{2})|^2. \tag{1}$$

Such final-state polarized partial widths are observables and, indeed, the equivalent helicity parameters $\xi,\sigma\ldots$, can be measured by various polarimetry and spin-correlation techniques.

The second helicity parameter is the b quark's chirality parameter $\xi\equiv(\Gamma_L^- + \Gamma_T^-)/\Gamma$. Equivalently,

$$\xi\equiv(\text{probability } b \text{ is } b_L)-(\text{probability } b \text{ is } b_R),$$

$$\xi\equiv|\langle b_L|b\rangle|^2-|\langle b_R|b\rangle|^2. \tag{2}$$

So for $m_b=0$, a value $\xi=1$ means the coupled b quark is pure b_L, i.e., $\lambda_b=-1/2$. For $m_b=4.5$ GeV, $\xi=0.9993$ for a pure $V-A$ coupling [6].

The remaining two partial-width parameters are defined by

$$\zeta\equiv(\Gamma_L^- - \Gamma_T^-)/\Gamma,\quad \sigma\equiv(\Gamma_L^+ - \Gamma_T^+)/\Gamma. \tag{3}$$

*Electronic address: cnelson@bingvmb.cc.binghamton.edu

This implies for W^+ polarimetry that

$$\sigma=(\text{probability } W^+ \text{ is } W_L)-(\text{probability } W^+ \text{ is } W_T)$$

is the analogue of the b quark's chirality parameter in Eq. (2). Thus the parameter σ measures the degree of polarization, ''L minus T,'' of the emitted W^+. For a pure $(V-A)$ or $(V+A)$ coupling and the empirical masses, $\sigma=0.4057$ so in the standard model (SM) about 70% of the final W's would be longitudinally polarized. The ''pre-spontaneous-supersymmetry-breaking (SSB)'' parameter $\zeta=0.4063$ (SM value) characterizes the remaining odd-odd mixture of the b and W^+ spin polarizations.

To describe the interference between the W_L and W_R amplitudes, we define the four normalized parameters:

$$\omega\equiv I_{\mathcal{R}}^-/\Gamma, \quad \eta\equiv I_{\mathcal{R}}^+/\Gamma,$$
$$\omega'\equiv I_{\mathcal{I}}^-/\Gamma, \quad \eta'\equiv I_{\mathcal{I}}^+/\Gamma. \tag{4}$$

The associated W_L-W_T interference intensities are

$$I_{\mathcal{R}}^{\pm}=|A(0,-\tfrac{1}{2})||A(-1,-\tfrac{1}{2})|\cos\beta_a \pm|A(0,\tfrac{1}{2})||A(1,\tfrac{1}{2})|\cos\beta_a^R,$$
$$I_{\mathcal{I}}^{\pm}=|A(0,-\tfrac{1}{2})||A(-1,-\tfrac{1}{2})|\sin\beta_a \pm|A(0,\tfrac{1}{2})||A(1,\tfrac{1}{2})|\sin\beta_a^R. \tag{5}$$

Here $\beta_a\equiv\phi_{-1}^a-\phi_0^a$ and $\beta_a^R\equiv\phi_1^a-\phi_0^{aR}$ are the measurable phase differences of the associated helicity amplitudes $A(\lambda_{W^+},\lambda_b)=|A|\exp\iota\phi$ in the standard helicity amplitude phase convention [4]. In the SM and for the empirical masses, $\omega=0.4566$ and $\eta=0.4568$ are unequal since $m_b=4.5$ GeV. If unlike in the SM $\beta_a^R\neq0$, then from Eq. (5) there are the inequalities $\omega'\neq\eta'$ and $\omega\neq\eta$, but both of these inequalities will be insignficant versus anticipated empirical precisions unless both b_R amplitudes, $\lambda_W=0,1$, are unexpectedly enhanced.

If one factors out ''W-polarimetry factors'' (see below) via $\sigma=\mathcal{S}_W\tilde{\sigma}$, $\omega=\mathcal{R}_W\tilde{\omega}$,..., the parameters all equal one or zero for a pure $(V-A)$ coupling and $m_b=0$ $(\omega'=\eta'=0)$.

A. Important remarks

(1) The analytic forms of ''$\xi,\sigma,\zeta,\ldots$'' are very distinct for different unique Lorentz couplings; see Table I. This is also true for the partial-width intensities for polarized final states; see Table II. This is indicative of the analyzing power of stage-two spin-correlation techniques for analyzing $t\to W^+b$ decay. Both the real and imaginary parts of the associated helicity amplitudes can be directly measured.

(2) Primed parameters $\omega'\neq0$ and/or $\eta'\neq0\Rightarrow\widetilde{T}_{FS}$ is violated. $\widetilde{T}_{FS}$ invariance will be violated when either there is a violation of canonical T invariance or when there are absorptive final-state interactions.

(3) Barred parameters $\bar{\xi},\bar{\zeta},\ldots$ have the analogous definitions for the CP conjugate process $\bar{t}\to W^-\bar{b}$. Therefore, any $\xi\neq\bar{\xi}$, $\zeta\neq\bar{\zeta}$, $\ldots\Rightarrow CP$ is violated. That is, ''slashed parameters'' $\not{\xi}\equiv\xi-\bar{\xi},\ldots$ could be introduced to characterize and quantify the degree of CP violation. This should be regarded as a test for the presence of a non-CKM-type CP violation because, normally, a CKM phase will contribute equally at the tree level to both the $t\to W^+b_L$ decay amplitudes and so a CKM phase will cancel out in the ratio of their moduli and in their relative phase. There are four tests for non-CKM-type CP violation [6,11].

(4) These helicity parameters appear in the general angular distributions for the polarized $t\to W^+b\to(l^+\nu)b$ decay chain and for $t\to W^+b\to(j\bar{d}j_u)b$. Such formulas for the associated ''stage-two spin-correlation'' (S2SC) functions in terms of these eight helicity parameters are derived below in Sec. V.

(5) In the presence of additional Lorentz structures, ''W-polarimetry factors'' $\mathcal{S}_W=0.4068$ and $\mathcal{R}_W=0.4567$

TABLE I. Analytic form of the helicity parameters for $t\to W^+b$ decay for unique Lorentz couplings: In this and the following table, the mass ratios are denoted by $w/t\equiv m_w/m_t$. We do not tabulate ω' and η' because $\omega'=\eta'=0$ if either (i) there is a unique Lorentz coupling, (ii) there is no $\widetilde{T}_{FS}$ violation, and/or (iii) there is a ''V and A, $m_b=0$'' masking mechanism; see remark (5) in Sec. I. $\mathcal{S}_W$ and $\mathcal{R}_W$ are given in Eqs. (6) and (7).

	$V\mp A$	$S\pm P$	f_M+f_E	f_M-f_E
Γ's				
ξ	±1	±1	1	-1
ζ	$\pm\mathcal{S}_W$	±1	$\dfrac{-2+w^2/t^2}{2+w^2/t^2}$	$+\frac{1}{3}$
σ	$\mathcal{S}_W$	1	$\dfrac{-2+w^2/t^2}{2+w^2/t^2}$	$-\frac{1}{3}$
Γ_{LT}'s				
ω	$\pm\mathcal{R}_W$	0	$\dfrac{\sqrt{2}w/t}{2+w^2/t^2}$	$-\dfrac{\sqrt{2}w}{3t}$
η	$\mathcal{R}_W$	0	$\dfrac{\sqrt{2}w/t}{2+w^2/t^2}$	$\dfrac{\sqrt{2}w}{3t}$

TABLE II. Analytical forms and numerical values of the partial-width intensities for polarized final states for unique Lorentz couplings.

	$V\mp A$	$S\pm P$	f_M+f_E	f_M-f_E
Analytic form				
Γ_L^-/Γ	$\pm\frac{1}{2}(1+\mathcal{S}_W)$	±1	$\dfrac{w^2}{2t^2+w^2}$	$-\frac{1}{3}$
Γ_T^-/Γ	$\pm\frac{1}{2}(1-\mathcal{S}_W)$	0	$\dfrac{2t^2}{2t^2+w^2}$	$-\frac{2}{3}$
Γ_L^+/Γ	$\frac{1}{2}(1+\mathcal{S}_W)$	1	$\dfrac{w^2}{2t^2+w^2}$	$+\frac{1}{3}$
Γ_T^+/Γ	$\frac{1}{2}(1-\mathcal{S}_W)$	0	$\dfrac{2t^2}{2t^2+w^2}$	$+\frac{2}{3}$
Numerical value				
Γ_L^-/Γ	±0.70	±1	0.095	-0.33
Γ_T^-/Γ	±0.30	0	0.905	-0.67
Γ_L^+/Γ	0.70	1	0.095	$+0.33$
Γ_T^+/Γ	0.30	0	0.905	$+0.67$

naturally appear [5,10] because of the referencing of ''new physics'' to the $(V-A)$ structure of the standard model (SM). These important factors are

$$\mathcal{S}_W=\frac{1-2m_W^2/m_t^2}{1+2m_W^2/m_t^2} \tag{6}$$

and

$$\mathcal{R}_W=\frac{\sqrt{2}m_W/m_t}{1+2m_W^2/m_t^2}. \tag{7}$$

We have introduced $\mathcal{S}_W$ and $\mathcal{R}_W$ because we are analyzing versus a reference $J_{b\bar{t}}$ theory consisting of ''a mixture of only V and A couplings with $m_b=0$.'' For the third generation of quarks and leptons, this is the situation in the SM before the Higgs mechanism is invoked. We refer to this limit as the ''pre-SSB'' case. In this case, these W-polarimetry factors have a simple physical interpretation: for $t\to W^+_{L,T}b$ the factor $\mathcal{S}_W=(\text{prob } W_L)-(\text{prob } W_T)$ and the factor $\mathcal{R}_W=$the ''geometric mean of these probabilities''$=\sqrt{(\text{prob } W_L)(\text{prob } W_T)}$. These factors are not independent since $\mathcal{S}_W^2+4\mathcal{R}_W^2=1$. [If experiments for the lighter quarks and leptons had suggested instead a different dominant Lorentz structure than $V-A$, say, ''f_M+f_E,'' then per Table I we would have replaced $\mathcal{S}_W$ everywhere by $(-2+w^2/t^2)/(2+w^2/t^2)$, etc.]

In the pre-SSB case, each of the eight helicity parameters also has a simple probabilistic significance for they are each directly proportional to Γ, ξ, $\mathcal{S}_W$, or $\mathcal{R}_W$: $\sigma\to\mathcal{S}_W$, $\zeta\to\mathcal{S}_W\xi$, $\omega\to\mathcal{R}_W\xi$, $\eta\to\mathcal{R}_W$. *Therefore,* precision measurements with ζ and ξ distinct, and with ξ and ω distinct, *will be two useful probes* of the dynamics of EW spontaneous symmetry breaking, see Eqs. (26–27) in Ref. 6. Some systematic effects will cancel by considering the ratios, ζ/ξ versus $\mathcal{R}_W$, and ω/ξ versus $\mathcal{S}_W$.

Note in this reference theory $\xi=(|g_L|^2-|g_R|^2)/(|g_L|^2+|g_R|^2)$. $\Gamma=q_W/4\pi(|g_L|^2+|g_R|^2)|V_{tb}|^2(m_t^2/m_w^2+1-2m_w^2/m_t^2)$ where $g_{L,R}=\frac{1}{2}(g_V\pm g_A)$, so in SM limit $g_L=g/2\sqrt{2}=g_V=-g_A$. Note also that any $\tilde{T}_{FS}$ violation is ''masked'' since $\omega'=\eta'=0$ (i.e., $\beta^a=\beta^b=0$) automatically. This ''V and A, $m_b=0$'' masking mechanism could be partially the cause for why T violation has not been manifest in previous experiments with the lighter quarks and leptons, even if it is not suppressed in the fundamental electroweak Lagrangian.

(6) The ''additional structure'' due to additional Lorentz couplings in $J_{b\bar{t}}$ can show up experimentally because of its interference with the $(V-A)$ part which, we assume, arises as predicted by the SM.

(7) Besides model independence, a major open issue is whether or not there is an additional chiral coupling in the t quark's charged current. A chiral classification of additional structure is a natural phenomenological extension of the standard $\mathrm{SU}(2)_L\times\mathrm{U}(1)$ electroweak symmetry. The requirement of $\overline{u(p_b)}\to\overline{u(p_b)}\frac{1}{2}(1+\gamma_5)$ and/or $u(k_t)\to\frac{1}{2}(1-\gamma_5)u(k_t)$ invariance of the vector and axial current matrix elements $\langle b|v^\mu(0)|t\rangle$ and $\langle b|a^\mu(0)|t\rangle$ allows only g_L, g_{S+P}, $g_{S^-+P^-}$, $g_+=f_M+f_E$, and $\tilde{g}_+=T^+ +T_5^+$ couplings. From this $\mathrm{SU}(2)_L$ perspective, the relevant experimental question is, what are the best limits on such additional couplings? Similarly, $\overline{u(p_b)}\to\overline{u(p_b)}\frac{1}{2}(1-\gamma_5)$ and/or $u(k_t)\to\frac{1}{2}(1+\gamma_5)u(k_t)$ invariance selects the complementary set of g_R, g_{S-P}, $g_{S^--P^-}$, $g_-=f_M-f_E$, and $\tilde{g}_-=T^+-T_5^+$ couplings. The absence of $\mathrm{SU}(2)_R$ couplings is simply built into the standard model; it is not predicted by it. So in the near future, it will be important to ascertain the limits on such $\mathrm{SU}(2)_R$ couplings in t quark physics.

(8) In a separate paper [6], it has been reported that at the Tevatron percent level statistical uncertainties are typical for measurements of the helicity parameters ξ, ζ, σ, ω, and η. At the LHC, several mill level uncertainties are typical. These are also the sensitivity levels found for measurement of the polarized partial widths $\Gamma^{\pm}_{L,T}$ and for the non-CKM-type CP violation parameter $r_a=|A(-1,-\frac{1}{2})|/|A(0,-\frac{1}{2})|$ versus $r_b=|B(1,\frac{1}{2})|/|B(0,\frac{1}{2})|$. From I_4 [see Eq. (69) below], the η parameter (ω parameter) can best be measured at the Fermilab Tevatron [CERN Large Hadron Collider (LHC)]. However, by the use of additional variables [all of $\tilde{\theta}_1$, $\tilde{\phi}_1$, $\tilde{\theta}_2$, and $\tilde{\phi}_2$ as in Eq. (66)] in the stage-two step of the decay sequences where $W^{\pm}\to j_{\bar{d},d}j_{u,\bar{u}}$ or $l^{\pm}\nu$, we expect that these sensitivities would then be comparable to that for the other helicity parameters. Inclusion of additional variables should also improve the sensitivity to the CP violation parameter β_a which is at 33° (Tevatron) and 9.4° (LHC). In regard to effective mass scales for new physics exhibited by additional Lorentz couplings, 50–70 TeV effective-mass scales can be probed at the Tevatron and 110–750 TeV scales at the LHC. The cleanest measurement of these parameters would presumably be at a future e^-e^+ or $\mu^-\mu^+$ collider.

In Sec. II, we introduce the necessary helicity formalism for describing $t\to W^+b\to(l^+\nu)b$ and $t\to W^+b\to(j_{\bar{d}}j_u)b$.

In Sec. III, we list the $A(\lambda_{W^+},\lambda_b)$ helicity amplitudes for $t\to W^+b$ for the most general $J_{b\bar{t}}$ current. Next, the helicity parameters are expressed in terms of a ''$(V-A)+$ additional chiral coupling'' structure in the $J_{b\bar{t}}$ current. Two tables display the leading-order expressions for the helicity parameters when the various additional chiral couplings $(g_i/2\Lambda_i)$ are small relative to the standard $V-A$ coupling (g_L).

Section IV gives the inverse formulas for extracting the contribution of the longitudinal and transverse W's to the polarized partial widths $\Gamma_{L,T}$ and to the partial-width interference intensities $I_{R,I}$ from measured values for the helicity parameters. Expressions are also listed for extracting the phase differences β_a and β_a^R from measured values for the helicity parameters.

Section V gives the derivation of the full S2SC function for the production decay sequence $q\bar{q}$ or $gg\to t\bar{t}\to(W^+b)(W^-\bar{b})\to(l^+\nu b)(l^-\bar{\nu}\bar{b})$ or $(j_{\bar{d}}j_u b)(j_d j_{\bar{u}}\bar{b})$. Two simpler S2SC are then derived. Several figures show the $\cos\theta_1^t$ and $\cos\tilde{\theta}_1$ behavior of the elements of the integrated or ''reduced'' composite density matrix $\rho_{hh'}$. It is this behavior, i.e., the use of W decay-polarimetry, which is responsible for the enhanced sensitivity of the S2SC function I_4 versus the energy-energy spin-correlation function $I(E_{W^+},E_{W^-})$.

Section VI contains some additional remarks.

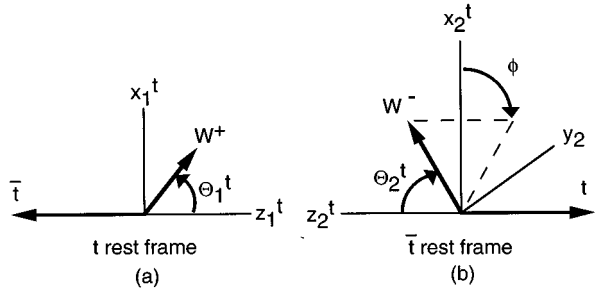

FIG. 1. The three angles θ_1^t, θ_2^t, and ϕ describe the first stage in the sequential decays of the $(t\,\bar{t}\,)$ system in which $t\to W^+b$ and $\bar{t}\to W^-\bar{b}$. From (a) a boost along the negative z_1^t axis transforms the kinematics from the t_1 rest frame to the $(tt)_{\rm c.m.}$ frame and, if boosted further, to the t_2 rest frame shown in (b).

II. HELICITY FORMALISM FOR $t\to W^+b\to(l^+\nu)b$ AND $t\to W^+b\to(j_{\bar{d}}j_u)b$

In the t rest frame, the matrix element for $t\to W^+b$ is

$$\langle\theta_1^t,\phi_1^t,\lambda_{W^+},\lambda_b|\tfrac{1}{2},\lambda_1\rangle=D^{(1/2)*}_{\lambda_1,\mu}(\phi_1^t,\theta_1^t,0)A(\lambda_{W^+},\lambda_b),\tag{8}$$

where $\mu=\lambda_{W^+}-\lambda_b$ and λ_1 is the t helicity. The final W^+ momentum is in the θ_1^t,ϕ_1^t direction; see Fig. 1. For the CP-conjugate process $\bar{t}\to W^-\bar{b}$ in the $\bar{t}$ rest frame,

$$\langle\theta_2^t,\phi_2^t,\lambda_{W^-},\lambda_{\bar{b}}|\tfrac{1}{2},\lambda_2\rangle=D^{(1/2)*}_{\lambda_2,\mu}(\phi_2^t,\theta_2^t,0)B(\lambda_{W^-},\lambda_{\bar{b}}),\tag{9}$$

with $\mu=\lambda_{W^-}-\lambda_{\bar{b}}$ and λ_2 is the $\bar{t}$ helicity. From Eqs. (8, 9) one sees that rotational invariance forbids the other transverse W^+ and W^- amplitudes, compare Eq. (1), and so there are only two, and not three, amplitudes $A(0,-1/2)$ and $A(-1,-1/2)$ for $t\to W^+b_L$, etc. An elementary, technical point [11] is that we have set the third Euler angle equal to zero in the large D functions in Eqs. (8) and (9). A nonzero value of the third Euler angle would imply an (awkward) associated rotation about the final W^+ momentum direction in Fig. 2. This technical point is important in this paper because in the spin correlation we exploit the azimuthal angular dependence of the second stage, $W^+\to l^+\nu$ or for $W^+\to j_{\bar{d}}j_u$, in the decay sequences.

Figure 2 defines the usual spherical angles $\tilde{\theta}_a$ and $\tilde{\phi}_a$ which specify the $j_{\bar{d}}$ jet (or the l^+) momentum in the W^+ rest frame when the boost is from the t rest frame. For the hadronic W^+ decay mode, we use the notation that the momentum of the charge $\frac{1}{3}e$ jet is denoted by $j_{\bar{d}}$ and the momentum of the charge $\frac{2}{3}e$ jet by j_u. Likewise, Fig. 3 defines the $\tilde{\theta}_b$ and $\tilde{\phi}_b$ which specify the j_d jet (or the l^-) momentum which occurs in the CP-conjugate decay sequence.

As shown in Fig. 4, we use subscripts ''1'' and ''2'' in place of ''a'' and ''b'' when the boost to these $W^\pm$ rest frames is directly from the $(t\,\bar{t}\,)_{\rm c.m.}$ center-of-mass frame. Physically, these angles, $\tilde{\theta}_a,\tilde{\phi}_a$ and $\tilde{\theta}_1,\tilde{\phi}_1$, are simply related by a Wigner rotation; see Eqs. (74) and (75) below. For the CP-conjugate mode, one only needs to change the subscripts $a\to b$ and $1\to 2$.

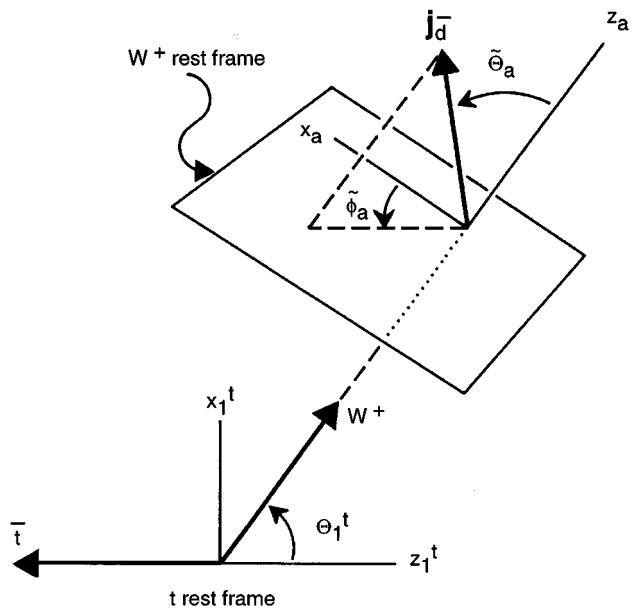

FIG. 2. The two pairs of spherical angles θ_1^t,ϕ_1^t and $\tilde{\theta}_a,\tilde{\phi}_a$ describe the respective stages in the sequential decay $t\to W^+b$ followed by $W^+\to j_{\bar{d}}j_u$ or $W^+\to l^+\nu$. The spherical angles $\tilde{\theta}_a$ and $\tilde{\phi}_a$ specify the $j_{\bar{d}}$ jet (or the l^+) momentum in the W^+ rest frame when the boost is from the t_1 rest frame. For the hadronic W^+ decay mode, we use the notation that the momentum of the charge $\frac{1}{3}e$ jet is denoted by $j_{\bar{d}}$ and the momentum of the charge $\frac{2}{3}e$ jet by j_u. In this figure, ϕ_1^t is shown equal to zero for simplicity of illustration.

In the W^+ rest frame, the matrix element for $W^+\to l^+\nu$ is [12,13]

$$\langle\tilde{\theta}_a,\tilde{\phi}_a,\lambda_{l^+},\lambda_\nu|1,\lambda_{W^+}\rangle=D^{1*}_{\lambda_{W^+},1}(\tilde{\phi}_a,\tilde{\theta}_a,0)c,\tag{10}$$

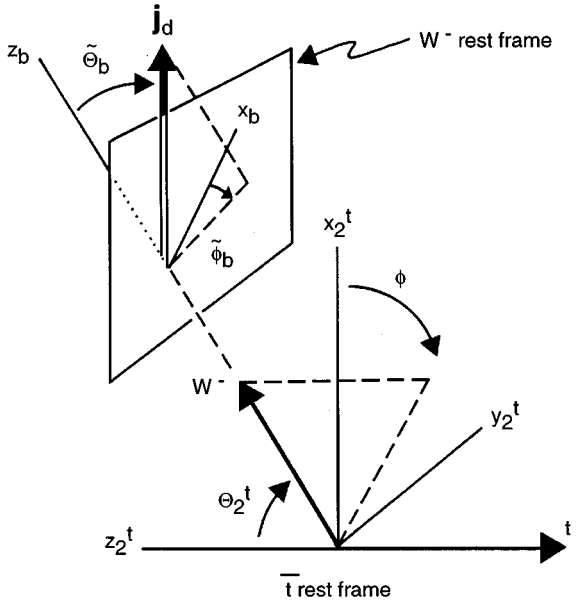

FIG. 3. This figure is symmetric versus Fig. 2. The spherical angles $\tilde{\theta}_b$ and $\tilde{\phi}_b$ specify the j_d jet (or the l^-) momentum in the W^- rest frame when the boost is from the $\bar{t}_2$ rest frame.

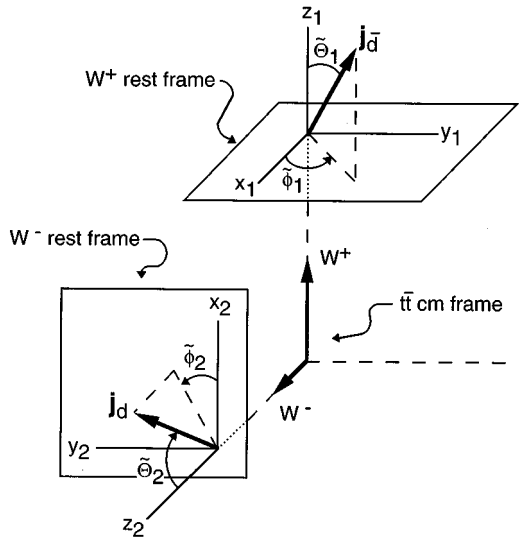

FIG. 4. The spherical angles $\tilde{\theta}_1$ and $\tilde{\phi}_1$ specify the $j\bar{d}$ jet (or the l^+) momentum in the W^+ rest frame when the boost is directly from the $(t\bar{t})_{\text{c.m.}}$ frame. Similarly, $\tilde{\theta}_2$ and $\tilde{\phi}_2$ specify the j_d jet (or the l^-) momentum in the W^- rest frame. The W^+W^- production half-plane specifies the positive x_1 and x_2 axes.

since $\lambda_\nu=-\frac{1}{2}$ and $\lambda_{l^+}=\frac{1}{2}$ neglecting (m_l/m_W) corrections. This equation also describes the $W^+\to j\bar{d}j_u$ decay mode, neglecting (m_{jet}/m_W) corrections.

The associated composite decay density matrix for $t\to W^+b\to(l^+\nu)b$ or for $t\to W^+b\to(j\bar{d}j_u)b$ is

$$R_{\lambda_1\lambda_1'}=\sum_{\lambda_W,\lambda_W'}\rho_{\lambda_1\lambda_1';\lambda_W\lambda_W'}(t\to W^+b)\rho_{\lambda_W\lambda_W'}(W^+\to l^+\nu), \tag{11}$$

where $\lambda_W,\lambda_W'=0,\pm1$, with

$$\begin{aligned}\rho_{\lambda_1\lambda_1';\lambda_W\lambda_W'}(t\to W^+b)=&\sum_{\lambda_b=\mp1/2}D^{(1/2)*}_{\lambda_1,\mu}(\phi_1^t,\theta_1^t,0)D^{(1/2)}_{\lambda_1',\mu'}\\&\times(\phi_1^t,\theta_1^t,0)A(\lambda_W,\lambda_b)\\&\times A(\lambda_W',\lambda_b)^*,\end{aligned}$$

$$\rho_{\lambda_W\lambda_W'}(W^+\to l^+\nu)=D^{1*}_{\lambda_W,1}(\tilde{\phi}_a,\tilde{\theta}_a,0)D^{1}_{\lambda_W',1}(\tilde{\phi}_a,\tilde{\theta}_a,0)|c|^2.$$

This composite decay density matrix can be expressed in terms of the eight helicity parameters:

$$\mathbf{R}=\begin{pmatrix}\mathbf{R}_{++}&e^{\iota\phi_1^t}\mathbf{r}_{+-}\\e^{-\iota\phi_1^t}\mathbf{r}_{-+}&\mathbf{R}_{--}\end{pmatrix}. \tag{12}$$

The diagonal elements are

$$\begin{aligned}\mathbf{R}_{\pm\pm}=&\mathbf{n}_a[1\pm\mathbf{f}_a\cos\theta_1^t]\pm(1/\sqrt{2})\sin\theta_1^t\{\sin2\tilde{\theta}_a[\omega\cos\tilde{\phi}_a\\&+\eta'\sin\tilde{\phi}_a]-2\sin\tilde{\theta}_a[\eta\cos\tilde{\phi}_a+\omega'\sin\tilde{\phi}_a]\}.\end{aligned} \tag{13}$$

The off-diagonal elements depend on

$$\begin{aligned}\mathbf{r}_{+-}=(\mathbf{r}_{-+})^*=&\mathbf{n}_a\mathbf{f}_a\sin\theta_1^t+\sqrt{2}\sin\tilde{\theta}_a\\&\times\{\cos\theta_1^t[\eta\cos\tilde{\phi}_a+\omega'\sin\tilde{\phi}_a]+\iota[\eta\sin\tilde{\phi}_a\\&-\omega'\cos\tilde{\phi}_a]\}-\frac{1}{\sqrt{2}}\sin2\tilde{\theta}_a\{\cos\theta_1^t[\omega\cos\tilde{\theta}_a+\eta'\sin\tilde{\theta}_a]\\&+i[\omega\sin\tilde{\theta}_a-\eta'\cos\tilde{\theta}_a]\}.\end{aligned} \tag{14}$$

In Eqs. (13) and (14),

$$\begin{aligned}\mathbf{n}_a=&\tfrac{1}{8}(5-\cos2\tilde{\theta}_a-\sigma[1+3\cos2\tilde{\theta}_a]-4[\xi-\zeta]\cos\tilde{\theta}_a),\\\mathbf{n}_a\mathbf{f}_a=&\tfrac{1}{8}(4[1-\sigma]\cos\tilde{\theta}_a-\xi[1+3\cos2\tilde{\theta}_a]\\&+\zeta[5-\cos2\tilde{\theta}_a]),\end{aligned} \tag{15}$$

or, equivalently,

$$\begin{pmatrix}\mathbf{n}_a\\\mathbf{n}_a\mathbf{f}_a\end{pmatrix}=\sin^2\tilde{\theta}_a\,\frac{\Gamma_L^\pm}{\Gamma}\pm\frac{1}{4}\,(3+\cos2\tilde{\theta}_a)\,\frac{\Gamma_T^\pm}{\Gamma}\mp\cos\tilde{\theta}_a\,\frac{\Gamma_T^\mp}{\Gamma}. \tag{16}$$

For the CP-conjugate process $\bar{t}\to W^-\bar{b}\to(l^-\bar{\nu})\bar{b}$ or $\bar{t}\to W^-\bar{b}\to(j_dj_{\bar{u}})\bar{b}$,

$$\bar{\mathbf{R}}=\begin{pmatrix}\bar{\mathbf{R}}_{++}&e^{\iota\phi_2^t}\bar{\mathbf{r}}_{+-}\\e^{-\iota\phi_2^t}\bar{\mathbf{r}}_{-+}&\bar{\mathbf{R}}_{--}\end{pmatrix}. \tag{17}$$

$$\begin{aligned}\bar{\mathbf{R}}_{\pm\pm}=&\mathbf{n}_b[1\mp\mathbf{f}_b\cos\theta_2^t]\mp(1/\sqrt{2})\sin\theta_2^t\{\sin2\tilde{\theta}_b[\bar{\omega}\cos\tilde{\phi}_b\\&-\bar{\eta}'\sin\tilde{\phi}_b]-\sin\tilde{\theta}_b[\bar{\eta}\cos\tilde{\phi}_b-\bar{\omega}'\sin\tilde{\phi}_b]\},\end{aligned} \tag{18}$$

$$\begin{aligned}\bar{\mathbf{r}}_{+-}=(\bar{\mathbf{r}}_{-+})^*=&-\mathbf{n}_b\mathbf{f}_b\sin\theta_2^t-\sqrt{2}\sin\tilde{\theta}_b\\&\times\{\cos\theta_2^t[\bar{\eta}\cos\tilde{\phi}_b-\bar{\omega}'\sin\tilde{\phi}_b]\\&+\iota[\bar{\eta}\sin\tilde{\phi}_b+\bar{\omega}'\cos\tilde{\phi}_b]\}+\frac{1}{\sqrt{2}}\sin2\tilde{\theta}_b\{\cos\theta_2^t[\bar{\omega}\cos\tilde{\phi}_b\\&-\bar{\eta}'\sin\tilde{\phi}_b]+i[\bar{\omega}\sin\tilde{\phi}_b+\bar{\eta}'\cos\tilde{\theta}_b]\},\end{aligned} \tag{19}$$

$$\begin{aligned}\mathbf{n}_b=&\tfrac{1}{8}(5-\cos2\tilde{\theta}_b-\bar{\sigma}[1+3\cos2\tilde{\theta}_b]-4[\bar{\xi}-\bar{\zeta}]\cos\tilde{\theta}_b),\\\mathbf{n}_b\mathbf{f}_b=&\tfrac{1}{8}(4[1-\bar{\sigma}]\cos\tilde{\theta}_b-\bar{\xi}[1+3\cos2\tilde{\theta}_b]\\&+\bar{\zeta}[5-\cos2\tilde{\theta}_b]).\end{aligned} \tag{20}$$

$$\begin{pmatrix}\mathbf{n}_b\\\mathbf{n}_b\mathbf{f}_b\end{pmatrix}=\sin^2\tilde{\theta}_b\,\frac{\bar{\Gamma}_L^\pm}{\bar{\Gamma}}\pm\frac{1}{4}\,(3+\cos2\tilde{\theta}_b)\,\frac{\bar{\Gamma}_T^\pm}{\bar{\Gamma}}\mp\cos\tilde{\theta}_b\,\frac{\bar{\Gamma}_T^\mp}{\bar{\Gamma}}. \tag{21}$$

III. HELICITY PARAMETERS IN TERMS OF CHIRAL COUPLINGS

For $t\to W^+b$, the most general Lorentz coupling is

$$W_\mu^*\bar{u}_b(p)\Gamma^\mu u_t(k), \tag{22}$$

where $k_t=q_w+p_b$. In Eq. (22),

$$\Gamma_V^\mu = g_V\gamma^\mu + \frac{f_M}{2\Lambda}\,\iota\sigma^{\mu\nu}(k-p)_\nu + \frac{g_{S^-}}{2\Lambda}\,(k-p)^\mu + \frac{g_S}{2\Lambda}\,(k+p)^\mu + \frac{g_{T^+}}{2\Lambda}\,\iota\sigma^{\mu\nu}(k+p)_\nu,$$

$$\Gamma_A^\mu = g_A\gamma^\mu\gamma_5 + \frac{f_E}{2\Lambda}\,\iota\sigma^{\mu\nu}(k-p)_\nu\gamma_5 + \frac{g_{P^-}}{2\Lambda}\,(k-p)^\mu\gamma_5 + \frac{g_P}{2\Lambda}\,(k+p)^\mu\gamma_5 + \frac{g_{T_5^+}}{2\Lambda}\,\iota\sigma^{\mu\nu}(k+p)_\nu\gamma_5.$$

The parameter $\Lambda=$ ''the effective-mass scale of new physics.''

Without additional theoretical or experimental inputs, it is not possible to select what is the ''best'' minimal set of couplings for analyzing the structure of the $J_{\overline{bt}}$ current. There are the ''equivalence theorems'' that for the vector current, $S\approx V+f_M$, $T^+\approx -V+S^-$, and for the axial-vector current, $P\approx -A+f_E$, $T_5^+\approx A+P^-$. On the other hand, dynamical considerations such as compositeness would suggest searching for an additional tensorial $g_+=f_M+f_E$ coupling which would preserve $\xi=1$, but otherwise give non-$(V-A)$ values to the t helicity parameters. For instance, $\sigma=\zeta\neq 0.41$ and $\eta=\omega\neq 0.46$.

The matrix elements of the divergences of these charged currents are

$$(k-p)_\mu V^\mu = \left[g_V(m_t-m_b) + \frac{g_{S^-}}{2\Lambda}\,q^2 + \frac{g_S}{2\Lambda}\,(m_t^2-m_b^2) + \frac{g_{T^+}}{2\Lambda}\,(q^2-[m_t-m_b]^2)\right]\overline{u_b}u_t, \tag{23}$$

$$(k-p)_\mu A^\mu = \left[-g_A(m_b+m_t) + \frac{g_{P^-}}{2\Lambda}\,q^2 + \frac{g_P}{2\Lambda}\,(m_t^2-m_b^2) + \frac{g_{T_5^+}}{2\Lambda}\,(q^2-[m_t+m_b]^2)\right]\overline{u_b}\gamma_5 u_t. \tag{24}$$

Both the weak magnetism $f_M/2\Lambda$ and the weak electricity $f_E/2\Lambda$ terms are divergenceless. On the other hand, since $q^2=m_w^2$, even when $m_b=m_t$ there are nonvanishing terms due to the couplings S^-, T^+, A, P^-, and T_5^+.

The modularity and simple symmetry relations [6] among the $t\to W^+b$ and $\overline{t}\to W^-\overline{b}$ amplitudes are possible because of the phase conventions that were built into the helicity formalism [4]. In combining these amplitudes with results from calculations of similar amplitudes by diagrammatic methods, care must be exercised to ensure that the same phase conventions are being used (cf. appendix in [11]).

The helicity amplitudes for $t\to W^+b_{L,R}$ for both $(V\mp A)$ couplings and m_b arbitrary are, for b_L and so $\lambda_b=-\frac{1}{2}$,

$$A(0,-\tfrac{1}{2}) = g_L\,\frac{E_w+q_w}{m_w}\,\sqrt{m_t(E_b+q_w)} - g_R\,\frac{E_w-q_w}{m_w}\,\sqrt{m_t(E_b-q_w)}, \tag{25}$$

$$A(-1,-\tfrac{1}{2}) = g_L\sqrt{2m_t(E_b+q_w)} - g_R\sqrt{2m_t(E_b-q_w)}, \tag{26}$$

and, for b_R and so $\lambda_b=\frac{1}{2}$,

$$A(0,\tfrac{1}{2}) = -g_L\,\frac{E_w-q_w}{m_w}\,\sqrt{m_t(E_b-q_w)} + g_R\,\frac{E_w+q_w}{m_w}\,\sqrt{m_t(E_b+q_w)}, \tag{27}$$

$$A(1,-\tfrac{1}{2}) = -g_L\sqrt{2m_t(E_b-q_w)} + g_R\sqrt{2m_t(E_b+q_w)}. \tag{28}$$

Note that g_L and g_R denote the ''chirality'' of the coupling and $\lambda_b=\mp\frac{1}{2}$ denote the handedness of $b_{L,R}$. For $(S\pm P)$ couplings, the additional contributions are

$$A(0,-\tfrac{1}{2}) = g_{S+P}\left(\frac{m_t}{2\Lambda}\right)\frac{2q_w}{m_w}\,\sqrt{m_t(E_b+q_w)} + g_{S-P}\left(\frac{m_t}{2\Lambda}\right)\frac{2q_w}{m_w}\,\sqrt{m_t(E_b-q_w)},$$

$$A(-1,-\tfrac{1}{2}) = 0, \tag{29}$$

$$A(0,\tfrac{1}{2}) = g_{S+P}\left(\frac{m_t}{2\Lambda}\right)\frac{2q_w}{m_w}\,\sqrt{m_t(E_b-q_w)} + g_{S-P}\left(\frac{m_t}{2\Lambda}\right)\frac{2q_w}{m_w}\,\sqrt{m_t(E_b+q_w)}, \quad A(1,\tfrac{1}{2}) = 0. \tag{30}$$

The two types of tensorial couplings $g_\pm=f_M\pm f_E$ and $\tilde{g}_\pm = g^+_{T^+\pm T_5^+}$ give the additional contributions

$$A(0,\mp\tfrac{1}{2}) = \mp g_+\left(\frac{m_t}{2\Lambda}\right)\left[\frac{E_w\mp q_w}{m_w}\,\sqrt{m_t(E_b\pm q_w)} - \frac{m_b}{m_t}\,\frac{E_w\mp q_w}{m_w}\,\sqrt{m_t(E_b\mp q_w)}\right] \pm g_-\left(\frac{m_t}{2\Lambda}\right)\left[-\frac{m_b}{m_t}\,\frac{E_w\pm q_w}{m_w}\,\sqrt{m_t(E_b\pm q_w)} + \frac{E_w\pm q_w}{m_w}\,\sqrt{m_t(E_b\mp q_w)}\right] \mp \tilde{g}_+\left(\frac{m_t}{2\Lambda}\right)\left[\frac{E_w\pm q_w}{m_w}\,\sqrt{m_t(E_b\pm q_w)} + \frac{m_b}{m_t}\,\frac{E_w\mp q_w}{m_w}\,\sqrt{m_t(E_b\mp q_w)}\right] \pm \tilde{g}_-\left(\frac{m_t}{2\Lambda}\right) \times\left[\frac{m_b}{m_t}\,\frac{E_w\pm q_w}{m_w}\,\sqrt{m_t(E_b\pm q_w)} + \frac{E_w\mp q_w}{m_w}\,\sqrt{m_t(E_b\mp q_w)}\right],$$

$$A(\mp 1,\mp\tfrac{1}{2}) = \mp\sqrt{2}g_+\left(\frac{m_t}{2\Lambda}\right)\left[\sqrt{m_t(E_b\pm q_w)} - \frac{m_b}{m_t}\sqrt{m_t(E_b\mp q_w)}\right] \pm \sqrt{2}g_-\left(\frac{m_t}{2\Lambda}\right)\left[-\frac{m_b}{m_t}\sqrt{m_t(E_b\pm q_w)} + \sqrt{m_t(E_b\mp q_w)}\right]$$

$$\mp\sqrt{2}\tilde{g}_+\left(\frac{m_t}{2\Lambda}\right)\left[\sqrt{m_t(E_b\pm q_w)} + \frac{m_b}{m_t}\sqrt{m_t(E_b\mp q_w)}\right] \pm \sqrt{2}\tilde{g}_-\left(\frac{m_t}{2\Lambda}\right)\left[\frac{m_b}{m_t}\sqrt{m_t(E_b\pm q_w)} + \sqrt{m_t(E_b\mp q_w)}\right]. \quad (31)$$

A. Helicity parameter form in terms of g_L plus one ''additional chiral coupling''

We first display the expected forms for the above helicity parameters for the $t\to W^+b$ decay for the case of a pure $V-A$ chiral coupling as in the SM. Next, we will give the form for the case of a single chiral coupling $(g_i/2\Lambda_i)$ in addition to the standard $V-A$ coupling. In this case, we first list the formulas for an arbitrarily large additional contribution.

In Tables III and IV we list the formulas to leading order in g_i versus the standard g_L coupling. Throughout this paper, we usually suppress the entry in the ''i'' subscript on the new physics coupling scale ''Λ_i'' when it is obvious from the context of interest.

In the case of ''multiadditional'' chiral contributions, the general formulas for $A(\lambda_{W^+},\lambda_b)$, which are listed above, can be substituted into the above definitions so as to derive the expression(s) for the ''multiadditional'' chiral contributions. The m_b/m_w and m_b/m_t corrections to the following expressions can similarly be included.

Pure $V-A$ coupling:

$$\xi=\sigma/\mathcal{S}_W=\zeta/\mathcal{S}_W=\omega/\mathcal{R}_W=\eta/\mathcal{R}_W=1,$$

$$\omega'=\eta'=0. \quad (32)$$

$V+A$ also present:

$$\zeta/\mathcal{S}_W=\xi, \quad \omega/\mathcal{R}_W=\xi,$$

$$\sigma/\mathcal{S}_W=1, \quad \eta/\mathcal{R}_W=1,$$

$$\xi=\frac{|g_L|^2-|g_R|^2}{|g_L|^2+|g_R|^2}, \quad \omega'=\eta'=0. \quad (33)$$

TABLE III. Helicity parameters for $t\to W^+b$ decay to leading order in the case of a single additional chiral coupling (g_i) which is small relative to the standard $V-A$ coupling (g_L). This table is for the $V+A$ and for the $S\pm P$ couplings. The next table (Table IV) is for additional tensorial couplings. In this paper Re (Im) denote, respectively, the real (imaginary) parts of the quantity inside the parentheses. Expressions for ''$a,\ldots,f$'' are given in Eq. (50).

	$V\pm A$		Additional $S\pm P$	
	Pure g_L	Plus g_R	Plus g_{S+P}	Plus g_{S-P}
Γ's				
ξ	1	$\frac{\lvert g_L\rvert^2-\lvert g_R\rvert^2}{\lvert g_L\rvert^2+\lvert g_R\rvert^2}$	1	$1-2e\left\lvert\frac{g_{S-P}}{g_L}\right\rvert^2$
$\zeta/\mathcal{S}_W$	1	ξ	$1+\frac{a\mathrm{Re}(g_L^*g_{S+P})+c\lvert g_{S+P}\rvert^2}{\lvert g_L\rvert^2}$	$1-b\left\lvert\frac{g_{S-P}}{g_L}\right\rvert^2$
$\sigma/\mathcal{S}_W$	1	1	$\zeta/\mathcal{S}_W$	$1+c\left\lvert\frac{g_{S-P}}{g_L}\right\rvert^2$
Γ_{LT}'s				
$\omega/\mathcal{R}_W$	1	ξ	$1-d\frac{\mathrm{Re}(g_L^*g_{S+P})+e\lvert g_{S+P}\rvert^2}{\lvert g_L\rvert^2}$	$1-e\left\lvert\frac{g_{S-P}}{g_L}\right\rvert^2$
$\eta/\mathcal{R}_W$	1	1	$\omega/\mathcal{R}_W$	$\omega/\mathcal{R}_W$
$\omega'/\mathcal{R}_W$	0	0	$-f\frac{\mathrm{Im}(g_L^*g_{S+P})}{\lvert g_L\rvert^2}$	0
$\eta'/\mathcal{R}_W$	0	0	$\omega'/\mathcal{R}_W$	0

TABLE IV. Same as Table III except this table is for additional tensorial couplings. Here $g_\pm = f_M \pm f_E$ involves $k_t - p_b$, whereas $\tilde{g}_\pm = g^+_{T^+ \pm T_5^+}$ involves $k_t + p_b$; see Eq. (22). Here m_t = mass of the t quark. Expressions for "$f,\ldots,u$" are given in Eq. (50) and (51).

	Additional $f_M \pm f_E$		Additional $T^+ \pm T_5^+$	
	Plus g_+	Plus g_-	Plus $\tilde{g}_+$	Plus $\tilde{g}_-$
Γ's				
ξ	1	$1-k\left\|\frac{g_-}{g_L}\right\|^2$	1	$\frac{\|g_L\|^2-\|m_t\tilde{g}_-/2\Lambda\|^2}{\|g_L\|^2+\|m_t\tilde{g}_-/2\Lambda\|^2}$
$\zeta/\mathcal{S}_W$	$1+\frac{g\,\mathrm{Re}(g_L^* g_+)-u\,\mathrm{Im}(g_L^* g_+)}{\|g_L\|^2}$	$1-h\left\|\frac{g_-}{g_L}\right\|^2$	1	ξ
$\sigma/\mathcal{S}_W$	$\zeta/\mathcal{S}_W$	$1-j\left\|\frac{g_-}{g_L}\right\|^2$	1	1
Γ_{LT}'s				
$\omega/\mathcal{R}_W$	$1-\frac{2l\,\mathrm{Re}(g_L^* g_+)+o\,\mathrm{Im}(g_L^* g_+)}{2\|g_L\|^2}$	$1-n\left\|\frac{g_-}{g_L}\right\|^2$	1	ξ
$\eta/\mathcal{R}_W$	$\omega/\mathcal{R}_W$	$1-o\left\|\frac{g_-}{g_L}\right\|^2$	1	1
$\omega'/\mathcal{R}_W$	$-f\frac{\mathrm{Im}(g_L^*+g_+)}{\|g_L\|^2}$	0	0	0
$\eta'/\mathcal{R}_W$	$\omega'/\mathcal{R}_W$	0	0	0

$S+P$ also present:

$$\zeta=\sigma=\left(\begin{array}{c}\left(1-2\frac{m_w^2}{m_t^2}\right)|g_L|^2+\frac{m_t}{\Lambda}\left[1-\frac{m_w^2}{m_t^2}\right]\mathrm{Re}(g_L^* g_{S+P}) \\ +\left\{\frac{m_t}{2\Lambda}\left[1-\frac{m_w^2}{m_t^2}\right]\right\}^2|g_{S+P}|^2\end{array}\right)\Big/(\mathcal{D}^+), \tag{34}$$

$$\xi=1, \tag{35}$$

$$\omega=\eta=\sqrt{2}\,\frac{m_w}{m_t}\left(|g_L|^2+\frac{m_t}{2\Lambda}\left[1-\frac{m_w^2}{m_t^2}\right]\mathrm{Re}(g_L^* g_{S+P})\right)\Big/(\mathcal{D}^+),$$

$$\omega'=\eta'=-\sqrt{2}\,\frac{m_w}{2\Lambda}\left[1-\frac{m_w^2}{m_t^2}\right]\mathrm{Im}(g_L^* g_{S+P})/(\mathcal{D}^+). \tag{36}$$

where

$$\mathcal{D}^+=\left(1+2\frac{m_w^2}{m_t^2}\right)|g_L|^2+\frac{m_t}{\Lambda}\left[1-\frac{m_w^2}{m_t^2}\right]\mathrm{Re}(g_L^* g_{S+P})+\left\{\frac{m_t}{2\Lambda}\left[1-\frac{m_w^2}{m_t^2}\right]\right\}^2|g_{S+P}|^2.$$

$S-P$ also present:

$$\zeta,\sigma=\left(\left(1-2\frac{m_w^2}{m_t^2}\right)|g_L|^2\mp\left\{\frac{m_t}{2\Lambda}\left[1-\left(\frac{m_w^2}{m_t^2}\right)\right]\right\}^2|g_{S-P}|^2\right)\Big/(\mathcal{D}^-), \tag{37}$$

where the upper (lower) sign on the right-hand side (RHS) goes with the first (second) entry on the left-hand side (LHS):

$$\xi=\left[\left(1+2\frac{m_w^2}{m_t^2}\right)|g_L|^2-\left\{\frac{m_t}{2\Lambda}\left[1-\left(\frac{m_w^2}{m_t^2}\right)\right]\right\}^2|g_{S-P}|^2\right]\Big/ (\mathcal{D}^-) \tag{38}$$

$$\omega=\eta=\sqrt{2}\,\frac{m_w}{m_t}\,|g_L|^2\Big/(\mathcal{D}^-),\quad \omega'=\eta'=0, \tag{39}$$

where

$$\mathcal{D}^-=\left(1+2\frac{m_w^2}{m_t^2}\right)|g_L|^2+\left\{\frac{m_t}{2\Lambda}\left[1-\frac{m_w^2}{m_t^2}\right]\right\}^2|g_{S-P}|^2.$$

f_M+f_E also present: For this case we write the coupling constant of the sum of the weak magnetism and the weak electricity couplings as

$$g_+=f_M+f_E.$$

In this notation,

$$\zeta=\sigma=\left(\left(1-2\frac{m_w^2}{m_t^2}\right)|g_L|^2+\frac{m_w^2}{m_t\Lambda}\,\mathrm{Re}(g_L^*g_+)+\frac{m_w^2}{4\Lambda^2}\left[-2+\frac{m_w^2}{m_t^2}\right]|g_+|^2\right)\Big/(\mathcal{D}_T^+), \tag{40}$$

$$\xi=1,$$

$$\omega=\eta=\sqrt{2}\,\frac{m_w}{m_t}\left(|g_L|^2-\frac{m_t}{2\Lambda}\left[1+\frac{m_w^2}{m_t^2}\right]\mathrm{Re}(g_L^*g_+)+\frac{m_w^2}{4\Lambda^2}|g_+|^2\right)\Big/(\mathcal{D}_T^+),$$

$$\omega'=\eta'=-\frac{m_w}{\sqrt{2}\Lambda}\left[1-\frac{m_w^2}{m_t^2}\right]\mathrm{Im}(g_L^*g_+)/(\mathcal{D}_T^+), \tag{41}$$

where

$$\mathcal{D}_T^+=\left(1+2\frac{m_w^2}{m_t^2}\right)|g_L|^2-3\frac{m_w^2}{m_t\Lambda}\,\mathrm{Re}(g_L^*g_+)+\frac{m_w^2}{4\Lambda^2}\left[2+\frac{m_w^2}{m_t^2}\right]|g_+|^2.$$

f_M-f_E also present: Similarly, we write the coupling constant of the difference of the weak magnetism and the weak electricity couplings as

$$g_-=f_M-f_E,$$

and so

$$\zeta,\sigma=\left[\left(1-2\frac{m_w^2}{m_t^2}\right)|g_L|^2\pm\frac{m_w^2}{4\Lambda^2}\,|g_-|^2\right]\Big/(\mathcal{D}_T^-), \tag{42}$$

where the upper (lower) sign on the RHS goes with the first (second) entry on the LHS. Also,

$$\xi=\left[\left(1+2\frac{m_w^2}{m_t^2}\right)|g_L|^2-3\frac{m_w^2}{4\Lambda^2}\,|g_-|^2\right]\Big/\mathcal{D}_T^-, \tag{43}$$

$$\omega,\eta=\sqrt{2}\,\frac{m_w}{m_t}\left(|g_L|^2\mp\frac{m_w^2}{4\Lambda^2}\,|g_-|^2\right)\Big/(\mathcal{D}_T^-),\quad \omega'=\eta'=0. \tag{44}$$

Here

$$\mathcal{D}_T^-=\left(1+2\frac{m_w^2}{m_t^2}\right)|g_L|^2+3\frac{m_w^2}{4\Lambda^2}\,|g_-|^2.$$

$T^+ + T_5^+$ also present: We let

$$\tilde{g}_+=g^+_{T+T_5}.$$

In this notation,

$$\zeta=\sigma=\xi=1. \tag{45}$$

Also,

$$\omega=\eta=1,\quad \omega'=\eta'=0. \tag{46}$$

A single additional $\tilde{g}_+=g^+_{T^++T_5^+}$ coupling does not change the values from that of the pure $V-A$ coupling.

$T^+ - T_5^+$ also present: We let

$$\tilde{g}_-=g^+_{T-T_5},$$

and so

$$\zeta=\xi,\quad \sigma=1, \tag{47}$$

$$\xi=\frac{|g_L|^2-|m_t\tilde{g}_-/2\Lambda|^2}{|g_L|^2+\left|\frac{m_t\tilde{g}_-}{2\Lambda}\right|^2}, \tag{48}$$

$$\omega=\xi,\quad \eta=1,\quad \omega'=\eta'=0. \tag{49}$$

A single additional $\tilde{g}_-=g^+_{T^+-T_5^+}$ coupling is equivalent to a single additional $V+A$ coupling, except for the interpretation of their respective chirality parameters.

B. Helicity parameters to leading order in one ''additional chiral coupling''

In Table III for the $V+A$ and for the $S\mp P$ couplings, we list the ''expanded forms'' of the above expressions to leading order in a single additional chiral coupling $(g_i/2\Lambda_i)$ versus the standard $V-A$ coupling (g_L). Similarly, in Table IV is listed the formulas for the additional tensorial couplings. The tensorial couplings include the sum and difference of the weak magnetism and electricity couplings, $g_\pm=f_M\pm f_E$, which involve the momentum difference $q_w=k_t-p_b$. The alternative tensorial couplings $\tilde{g}_\pm=g^+_{T^+\pm T_5^+}$ instead involve k_t+p_b. In application [6] of I_4 to determine limits on a pure $IM(g_+)$, as in [6], since $\mathrm{Re}(g_L{}^*g_+)=0$, the additional terms in Table IV going as $|g_+|^2$ can be used; for other than pure $\mathrm{Im}(g_+)$, one should work directly from the above expressions in the text. This remark also applies for determination of limits for a pure $\mathrm{Im}(g_{S+P})$ from Table III.

Notice that, except for the following coefficients, the formulas tablulated in these two tables are short and simple. As above, we usually suppress the entry in the ''i'' subscript on ''Λ_i''. For Table III these coefficients are

$$a=\frac{4m_w^2}{m_t\Lambda}\frac{(1-m_w^2/m_t^2)}{(1-4m_w^4/m_t^4)},$$

$$d=\frac{m_t}{4\Lambda}\left(1-\frac{m_w^2}{m_t^2}\right)\frac{(1-2m_w^2/m_t^2)}{(1+2m_w^2/m_t^2)},$$

$$b=\frac{m_t^2}{2\Lambda^2}\frac{(1-m_w^2/m_t^2)^2}{(1-4m_w^4/m_t^4)},\quad e=\frac{m_t^2}{4\Lambda^2}\frac{(1-m_w^2/m_t^2)^2}{(1+2m_w^2/m_t^2)},$$

$$c=\frac{m_w^2}{\Lambda^2}\frac{(1-m_w^2/m_t^2)^2}{(1-4m_w^4/m_t^4)},\quad f=\frac{m_t}{2\Lambda}\left(1-\frac{m_w^2}{m_t^2}\right). \tag{50}$$

The coefficients for Table IV are

$$g=\frac{2m_w^2}{m_t\Lambda}\frac{(1-4m_w^2/m_t^2)}{(1-4m_w^4/m_t^4)},\quad l=\frac{m_t(1+9m_w^2/m_t^2+2m_w^4/m_t^4)}{2\Lambda(1+2m_w^2/m_t^2)},$$

$$h=\frac{m_w^2}{2\Lambda^2}\frac{(1-4m_w^2/m_t^2)}{(1-4m_w^4/m_t^4)},\quad n=\frac{m_w^2(2+m_w^2/m_t^2)}{2\Lambda^2(1+2m_w^2/m_t^2)},$$

$$j=\frac{m_w^2}{\Lambda^2}\frac{(1-m_w^2/m_t^2)}{(1-4m_w^4/m_t^4)},\quad o=\frac{m_w^2(1-m_w^2/m_t^2)}{2\Lambda^2(1+2m_w^2/m_t^2)},$$

$$k=\frac{3m_w^2}{2\Lambda^2(1+2m_w^2/m_t^2)},\quad u=\frac{m_w^2}{\Lambda^2}\frac{(1-m_w^4/m_t^4)}{(1-4m_w^4/m_t^4)}. \tag{51}$$

Notice that $O(1/\Lambda)$ coefficients occur in the case of an interference with the g_L coupling and that otherwise $O(1/\Lambda^2)$ coefficients occur.

When the experimental precision is sensitive to effects associated with the finite width ~ 2.07 GeV of the W boson, then a smearing over this width and a more sophisticated treated of these coefficients will be warranted. Numerically, for $m_t=175$ GeV, $m_w=80.36$ GeV, and $m_b=4.5$ GeV, these coefficients are

$$a\Lambda=141.6,\quad b\Lambda^2=11\,600,\quad c\Lambda^2=4890,$$

$$d\Lambda=14.05,\quad e\Lambda^2=3354,\quad f\Lambda=69.05,$$

$$g\Lambda=14.07,\quad h\Lambda^2=615.4,\quad j\Lambda^2=6197,$$

$$k\Lambda^2=6812,\quad l\Lambda=183.8,\quad n\Lambda^2=5020,$$

$$o\Lambda^2=1792,\quad u\Lambda^2=7503. \tag{52}$$

In comparing the entries in these two tables, notice that (i) a single additional $\tilde{g}_+=g^+_{T^++T_5^+}$ coupling does not change the values from that of the pure $V-A$ coupling and that (ii) a single additional $\tilde{g}_-=g^+_{T^+-T_5^+}$ coupling is equivalent to a single additional $V+A$ coupling, except for the interpretation of their respective chirality parameters. This follows as a consequence of the above ''equivalence theorems'' and the absence of contributions from the S^- and P^- couplings when the W^+ is on shell. We have displayed this equivalence in Table IV to emphasize that while an assumed total absence of $\tilde{g}_\pm$ couplings in $t\to W^+b$ decay might be supported by the weaker test of the experimental and theoretical normalization of the decay rate (i.e., the canonical universality test), empirical $V-A$ $(V+A)$ values of the helicity parameters shown in these tables will not imply the absence of $\tilde{g}_+$ $(\tilde{g}_-)$ couplings.

IV. TESTS FOR ''NEW PHYSICS''

In the context of the helicity parameters, this topic is discussed in a separate paper [6]. Here we include some useful formulas that were omitted in that discussion.

The contribution of the longitudinal (L) and transverse (T) W amplitudes in the decay process is projected out by the simple formulas

$$I_{\mathcal{R}}^{b_L,b_R}\equiv\frac{1}{2}(I_{\mathcal{R}}^+\pm I_{\mathcal{R}}^-)=\left|A\left(0,\mp\frac{1}{2}\right)\right|\left|A\left(\mp1,\mp\frac{1}{2}\right)\right|\cos\beta_a^{L,R}$$
$$=\frac{\Gamma}{2}(\eta\pm\omega),$$

$$I_{\mathcal{I}}^{b_L,b_R}\equiv\frac{1}{2}(I_{\mathcal{I}}^+\pm I_{\mathcal{I}}^-)=\left|A\left(0,\mp\frac{1}{2}\right)\right|\left|A\left(\mp1,\mp\frac{1}{2}\right)\right|\sin\beta_a^{L,R}$$
$$=\frac{\Gamma}{2}(\eta'\pm\omega'),$$

$$\Gamma_L^{b_L,b_R}\equiv\frac{1}{2}(I_L^+\pm I_L^-)=\left|A\left(0,\mp\frac{1}{2}\right)\right|^2=\frac{\Gamma}{4}(1+\sigma\pm\xi\pm\zeta),$$

$$\Gamma_T^{b_L,b_R} \equiv \frac{1}{2}(I_T^+ \pm I_T^-) = \left| A\left(\mp 1, \mp\frac{1}{2}\right)\right|^2 = \frac{\Gamma}{4}(1-\sigma \pm \xi \mp \zeta). \tag{53}$$

In the first line, $\beta_a^L = \beta_a$. Unitarity, requires the two right-triangle relations

$$(I_{\mathcal{R}}^{b_L})^2 + (I_{\mathcal{I}}^{b_L})^2 = \Gamma_L^{b_L}\Gamma_T^{b_L}, \tag{54}$$

$$(I_{\mathcal{R}}^{b_R})^2 + (I_{\mathcal{I}}^{b_R})^2 = \Gamma_L^{b_R}\Gamma_T^{b_R}. \tag{55}$$

It is important to determine directly from experiment whether or the W_L and W_T partial widths are anomalous in nature versus the standard $(V-A)$ predictions. They might have distinct dynamical differences versus the SM predictions if electroweak dynamical symmetry breaking (DSB) occurs in nature.

By unitarity and the assumption that only the minimal helicity amplitudes are needed, one can easily derive expressions for measuring the phase differences between the helicity amplitudes. In the case of both b_L and b_R couplings, there is

$$\cos\beta_a = \frac{I_{\mathcal{R}}^{b_L}}{\sqrt{\Gamma_L^{b_L}\Gamma_T^{b_L}}} = \frac{2(\omega+\eta)}{\sqrt{(1+\xi)^2-(\sigma+\zeta)^2}} \tag{56}$$

and, for the b_R phase difference,

$$\cos\beta_a^R = \frac{I_{\mathcal{R}}^{b_R}}{\sqrt{\Gamma_L^{b_R}\Gamma_T^{b_R}}} = \frac{2(\eta-\omega)}{\sqrt{(1-\xi)^2-(\sigma-\zeta)^2}}. \tag{57}$$

Also,

$$\sin\beta_a = \frac{I_{\mathcal{I}}^{b_L}}{\sqrt{\Gamma_L^{b_L}\Gamma_T^{b_L}}} = \frac{2(\omega'+\eta')}{\sqrt{(1+\xi)^2-(\sigma+\zeta)^2}}, \tag{58}$$

with

$$\sin\beta_a^R = \frac{I_{\mathcal{I}}^{b_R}}{\sqrt{\Gamma_L^{b_R}\Gamma_T^{b_R}}} = \frac{2(\eta'-\omega')}{\sqrt{(1-\xi)^2-(\sigma-\zeta)^2}}. \tag{59}$$

Measurement of $\beta_a \neq 0$ $(\beta_b \neq 0)$ implies a violation of T invariance in $t \to W^+ b$ $(\bar{t} \to W^- \bar{b})$ or the presence of an unexpected final-state interaction between the b and W^+. Because of the further assumption of no unusual final-state interactions, one is actually testing for $\tilde{T}_{FS}$ invariance. Canonical T invariance relates $t \to W^+ b$ and the actual time-reversed process $W^+ b \to t$, which is not directly accessible by present experiments. Equivalent to the two right-triangle relations are two expressions involving the helicity parameters:

$$(\eta \pm \omega)^2 + (\eta' \pm \omega')^2 + \tfrac{1}{4}[(1\pm\xi)^2 - (\sigma\pm\zeta)^2]. \tag{60}$$

Figure 5 displays a simple test of $\tilde{T}_{FS}$ invariance using the first relation. With forseeable experimental precisions, the second relation appears unlikely to be tested in the near future.

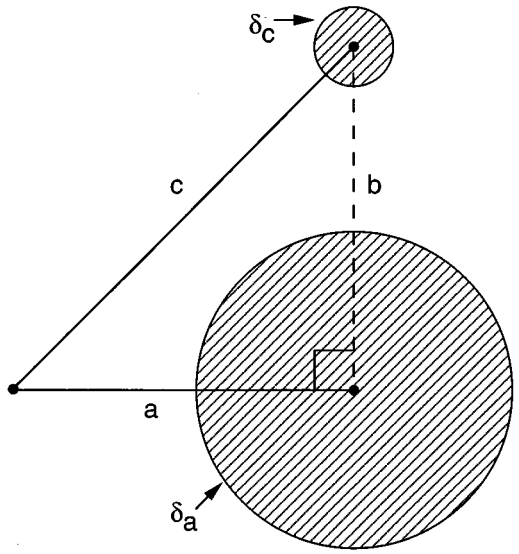

FIG. 5. Display of test for $\tilde{T}_{FS}$ violation using the right-triangle relation, Eq. (60): First, side $a = \eta + \omega$ is drawn with its uncertainty δ_a and then the hypotenuse $c = \frac{1}{2}\sqrt{[(1+\xi)^2-(\sigma+\zeta)^2]}$ is cast to form a right triangle. c's uncertainty is shown as δ_c. A resulting nonzero side $b = \eta' + \omega'$ would imply that $\tilde{T}_{FS}$ is violated either dynamically or because of a fundamental violation of canonical T invariance.

V. STAGE-TWO SPIN-CORRELATION FUNCTIONS

For $t\bar{t}$ production at hadron colliders, a simple consequence of the quantum-mechanical factorization structure of the parton model is that there are incident parton longitudinal beams characterized by the Feynman x_1 and x_2 momentum fractions instead of the known p and $\bar{p}(p)$ momenta. This momentum uncertainty must therefore be smeared over in application of the following S2SC functions and in determination [6] of the associated sensitivities for measurement of the above helicity parameters.

A. Full S2SC function

We consider the production-decay sequence

$$\begin{aligned} q\bar{q} \text{ or } gg \to t\bar{t} &\to (W^+ b)(W^- \bar{b}) \\ &\to (l^+ \nu b)(l^- \bar{\nu}\bar{b}) \quad \text{or} \quad (j_d \bar{j}_u b)(j_d \bar{j}_u \bar{b}). \end{aligned} \tag{61}$$

The general angular distribution in the $(t\bar{t})_{\text{c.m.}}$ is

$$\begin{aligned} &I(\Theta_B, \Phi_B; \theta_1^t, \phi_1^t; \tilde{\theta}_a, \tilde{\phi}_a; \theta_2^t, \phi_2^t; \tilde{\theta}_b, \tilde{\phi}_b) \\ &= \Sigma_{\lambda_1\lambda_2\lambda_1'\lambda_2'} \Big\{ \rho^{\text{prod}}_{\lambda_1\lambda_2;\lambda_1'\lambda_2'}(\Theta_B, \Phi_B) R_{\lambda_1\lambda_1'}(t \to W^+ b \to \dots) \\ &\quad \times \overline{R_{\lambda_2\lambda_2'}}(\bar{t} \to W^- \bar{b} \to \cdots) \Big\}, \end{aligned} \tag{62}$$

where the composite decay density matrix $R_{\lambda_1\lambda_1'}$ for $t \to W^+ b \to \cdots$ is given by Eq. (12) and that $R_{\lambda_2\lambda_2'}$ for

$\bar{t}\to W^-\bar{b}\to\cdots$ is given by Eq. (17). The angles Θ_B and Φ_B give [11,12] the direction of the incident parton beam, i.e., the q momentum or the gluon momentum, arising from the incident p in the $p\bar{p}$ or $pp\to t\bar{t}X$ production process. With Eq. (62) there is an associated differential counting rate

$$dN=I(\Theta_B,\Phi_B;\ldots)d(\cos\Theta_B)d\Phi_B D(\cos\theta_1^t)d\phi_1^t \times d(\cos\tilde{\theta}_a)d\tilde{\phi}_a d(\cos\theta_2^t)d\phi_2^t d(\cos\tilde{\theta}_b)d\tilde{\phi}_b, \quad (63)$$

where, for full phase space, the cosine of each polar angle ranges from -1 to 1 and each azimuthal angle ranges from 0 to 2π.

Each term in Eq. (62) can depend on the angle between the t and $\bar{t}$ decay planes

$$\phi=\phi_1^t+\phi_2^t \quad (64)$$

and on the angular difference

$$\Phi_R=\Phi_B-\phi_1^t. \quad (65)$$

So we treat Φ_B, Φ_R, and ϕ as the azimuthal variables. We integrate out Φ_R. The resulting full S2SC function is relatively simple:

$$\begin{aligned} &I(\Theta_B,\Phi_B;\phi;\theta_1^t,\tilde{\theta}_a,\tilde{\phi}_a;\theta_2^t,\tilde{\theta}_b,\tilde{\phi}_b) \\ &=\Sigma_{h_1h_2}\{\rho^{\rm prod}_{h_1h_2,h_1h_2}R_{h_1h_1}\overline{R_{h_2h_2}}+(\rho^{\rm prod}_{++,--}r_{+-}\overline{r_{+-}} \\ &\quad+\rho^{\rm prod}_{--,++}r_{-+}\overline{r_{-+}})\cos\phi+i(\rho^{\rm prod}_{++,--}r_{+-}\overline{r_{+-}} \\ &\quad-\rho^{\rm prod}_{--,++}r_{-+}\overline{r_{-+}})\sin\phi\}, \end{aligned} \quad (66)$$

where $\rho^{\rm prod}_{h_1h_2,h_1h_2}(\Theta_B,\Phi_B)$ still depends on Θ_B and Φ_B and the composite density matrix elements are given above. The θ_1^t angular dependence can be replaced by the W^+ energy in the $(t\bar{t})_{\rm c.m.}$ and similarly θ_2^t by the W^- energy [12]. The $\sin\phi$ dependence is the well-known test for CP violation in the production process [13,5].

B. Two simpler S2SC functions

We next integrate out some of the variables to obtain simpler S2SC functions. First [11], we transform to the variables of Fig. 4 and then integrate out the two azimuthal angles $\tilde{\phi}_{1,2}$. This gives a five-variable S2SC function with respect to the final decay products:

$$\begin{aligned} I(\phi;\theta_1^t,\tilde{\theta}_1,;\theta_2^t,\tilde{\theta}_2)=\Sigma_{h_1h_2}\{&\rho^{\rm prod}_{h_1h_2,h_1h_2}R_{h_1h_1}\overline{R_{h_2h_2}} \\ &+2\cos\phi\ {\rm Re}(\rho^{\rm prod}_{++,--}\rho_{+-}\overline{\rho_{+-}}) \\ &-2\sin\phi\ {\rm Im}(\rho^{\rm prod}_{++,--}\rho_{+-}\overline{\rho_{+-}})\}. \end{aligned} \quad (67)$$

The $\sin\phi$ term will vanish if both CP invariance holds in $(t\bar{t})$ production and $\beta_a=\beta_b=0$ in t and $\bar{t}$ decays. The dependence on $\Theta_B=\theta_t$, Φ_B, is implicit in Eqs. (67) and (69). Only θ_t appears in Eqs. (78)–(81) so the Φ_B integration is trivial for Eq. (69).

Diagonal $\rho_{\pm\pm}$ and off-diagonal $\rho_{\pm\mp}$ appear here to describe the decay sequence $t\to W^+b\to l^+\nu b$ or $j_{\bar{d}}\bar{j}_u b$. The

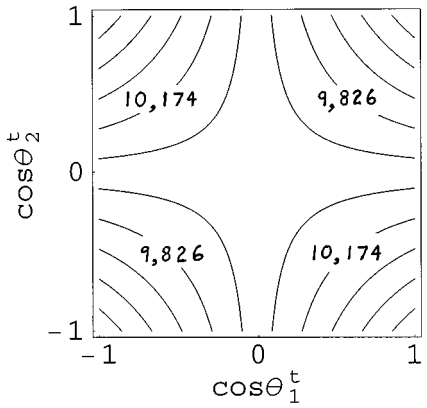

FIG. 6. Display of the W^+-energy–W^--energy correlation $I_2^{\rm c.m.}(\cos\theta_1^t,\cos\theta_2^t)$ as predicted by the standard model for $pp\to t\bar{t}X$ (LHC). The contours shown are for 10^6 events over 10 bins×10 bins (LHC). This saddle surface peaks at $(\pm1,\mp1)$, and the levels range from 9478 to 10 522 with spacing 116. [At the Tevatron at 2 TeV, the saddle is inverted with dips at $(\pm1,\mp1)$, with levels ranging from 294 to 306 with spacing 1.2 for 3×10^4 events.]

CP-conjugate sequences are described by $\overline{\rho_{\pm\pm}}$ and $\overline{\rho_{\pm\mp}}$. These integrated, composite density matrix elements are defined by

$$\rho_{h_1h_1}\equiv\frac{1}{2\pi}\int_0^{2\pi}d\phi_1 R_{h_1h_1}/|A(0,-\tfrac{1}{2})|^2,$$

$$\begin{aligned} \overline{\rho_{h_2h_2}}&\equiv\frac{1}{2\pi}\int_0^{2\pi}d\phi_1\overline{R_{h_2h_2}}/|B(0,\tfrac{1}{2})|^2 \\ &=\rho_{-h_2-h_2}({\rm subscripts}\ \ 1\to2,a\to b), \end{aligned}$$

$$\rho_{+-}=(\rho_{-+})^*\equiv\frac{1}{2\pi}\int_0^{2\pi}d\phi_1 r_{+-}/|A(0,-\tfrac{1}{2})|^2,$$

$$\begin{aligned} \overline{\rho_{+-}}=(\overline{\rho_{-+}})^*&\equiv\frac{1}{2\pi}\int_0^{2\pi}d\phi_1\overline{r_{+-}}/|B(0,\tfrac{1}{2})|^2 \\ &=-\rho_{+-}({\rm subscripts}\ \ 1\to2,a\to b,\beta_a\to\beta_b), \end{aligned} \quad (68)$$

where the last lines for the CP-conjugate ones shows useful CP substitution rules.

By integrating out the angle ϕ between the t and $\bar{t}$ decay planes, a simple four-variable S2SC function is obtained:

$$\begin{aligned} I(E_{W^+},E_{W^-},\tilde{\theta}_1,\tilde{\theta}_2)&=\Sigma_{h_1,h_2}\{\rho^{\rm prod}_{h_1h_2,h_1h_2}\rho_{h_1h_1}\overline{\rho_{h_2h_2}}\} \\ &=\Sigma_i\{\rho_{+-}(q_i\bar{q}_i\to t\bar{t})^{\rm prod}[\rho_{++}\overline{\rho_{--}} \\ &\quad+\rho_{--}\overline{\rho_{++}}]+\rho_{++}(gg\to t\bar{t})^{\rm prod} \\ &\quad\times[\rho_{++}\overline{\rho_{++}}+\rho_{--}\overline{\rho_{--}}]\}, \end{aligned} \quad (69)$$

where the sum is over the quarks and gluons in the incident $p\bar{p}$ or pp. In the second line we have assumed CP invariance in the production processes.

The simplest kinematic measurement of the above helicity parameters at the Tevatron and at the LHC would be through

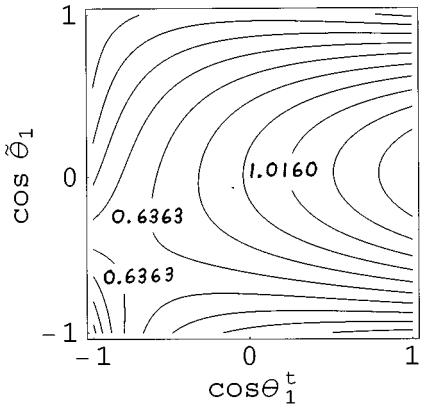

FIG. 7. First of eight figures showing the $\cos\theta_1^t,\cos\tilde{\theta}_1$ behavior of the elements of the ''reduced'' composite density matrix $\rho_{hh'}$. These also show the dependence as the total center-of-mass energy $E_{\text{c.m.}}$ of tt, in $(tt)_{\text{c.m.}}$, is changed. This figure is for ρ_{++} and $E_{\text{c.m.}}=380$ GeV; the next figure is for $E_{\text{c.m.}}=450$ GeV. This saddle surface peaks at about $(1,0),(-1,-1)$, and the levels range from 0.1300 to 1.3923 with spacing 0.1266.

purely hadronic top quark decay modes. The CDF and D0 Collaborations have reported [14] the observation of such decays. In this case the $(tt)_{\text{c.m.}}$ frame is accessible and the above I_4 can be used. In a separate paper [6] we have reported that the associated statistical sensitivities to the helicity parameters are at the percent level for measurements at the Tevatron and at the several mill level for the LHC. Figure 6 shows the net $E_{W^+}E_{W^-}$ dependence of Eq. (69).

C. Integrated composite decay density matrix elements

In Eq. (69), the composite decay density matrix elements are simply the decay probability for a t_1 with helicity $h/2$ to decay $t\to W^+b$ followed by $W^+\to j\bar{j}_u$ or $W^+\to l^+\nu$ since $dN/d(\cos\theta_1^t)d(\cos\tilde{\theta}_1)=\rho_{hh}(\theta_1^t,\tilde{\theta}_1)$ and, for the decay of the t_2 with helicity $h/2$, $\rho_{hh}=\rho_{-h,-h}$ $(1\to 2$, add bars). For t_1 with helicity $h/2$,

$$\rho_{hh}=\rho_0+h\rho_c\cos\theta_1^t+h\rho_s\sin\theta_1^t, \tag{70}$$

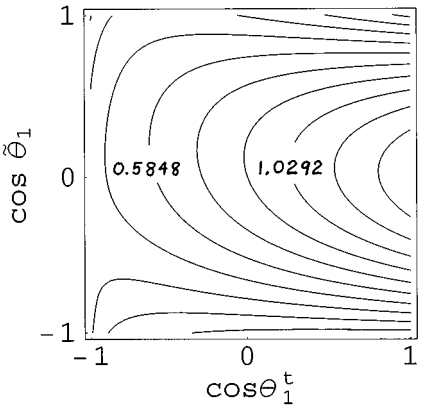

FIG. 8. The $\cos\theta_1^t,\cos\tilde{\theta}_1$ behavior of ρ_{++} for $E_{\text{c.m.}}=450$ GeV. The surface peaks at about $(1,0)$, and falls towards the three corners; the levels range from 0.1751 to 1.3422 with spacing 0.1220.

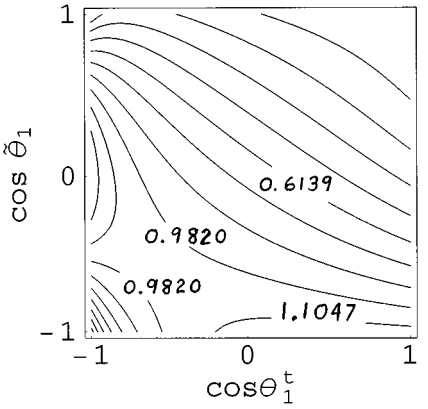

FIG. 9. The $\cos\theta_1^t,\cos\tilde{\theta}_1$ behavior of ρ_{--} for $E_{\text{c.m.}}=380$ GeV. The saddle surface peaks at about $(-1,0),(1,-1)$; the levels range from 0.1231 to 1.2274 with spacing 0.1227.

where

$$\rho_0=\tfrac{1}{8}\{6-2\cos^2\omega_1\cos^2\tilde{\theta}_1-\sin^2\omega_1\sin^2\tilde{\theta}_1+\sigma[2-6\cos^2\omega_1\cos^2\tilde{\theta}_1-3\sin^2\omega_1\sin^2\tilde{\theta}_1]-4(\xi-\zeta)\cos\omega_1\cos\tilde{\theta}_1\}, \tag{71}$$

$$\rho_c=\tfrac{1}{8}\{\zeta[6-2\cos^2\omega_1\cos^2\tilde{\theta}_1-\sin^2\omega_1\sin^2\tilde{\theta}_1]+\xi[2-6\cos^2\omega_1\cos^2\tilde{\theta}_1-3\sin^2\omega_1\sin^2\tilde{\theta}_1]+4(1-\sigma)\cos\omega_1\cos\tilde{\theta}_1\}, \tag{72}$$

$$\rho_s=\frac{1}{\sqrt{2}}\left\{\frac{1}{2}\omega\sin2\omega_1[\sin^2\tilde{\theta}_1-2\cos^2\tilde{\theta}_1]+2\eta\sin\omega_1\cos\tilde{\theta}_1\right\}, \tag{73}$$

with the Wigner rotation angle $\omega_1=\omega_1(E_{W^+})$. The rotation by ω_1 is about the implicit y_a axis in Fig. 2. It is given by [11]

$$\sin\omega_1=m_W\beta\gamma\sin\theta_1^t/p_1, \tag{74}$$

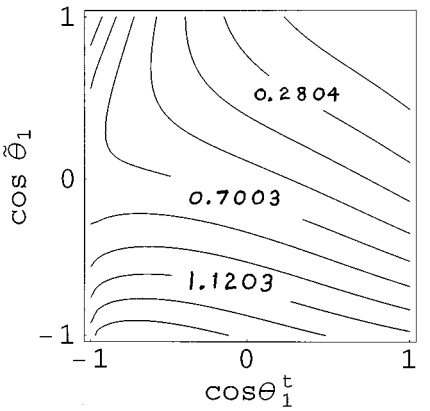

FIG. 10. The $\cos\theta_1^t,\cos\tilde{\theta}_1$ behavior of ρ_{--} for $E_{\text{c.m.}}=450$ GeV. The surface peaks at about $(-1,1)$, $(-0.5,-1)$; the levels range from 0.1404 to 1.4002 with spacing 0.1400.

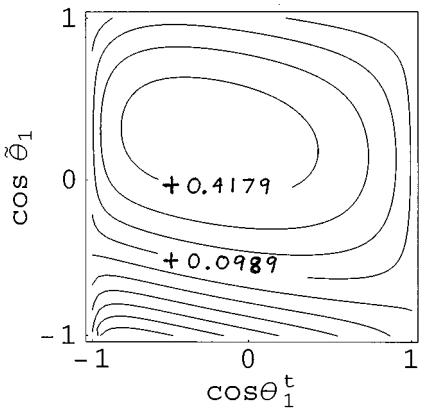

FIG. 11. The $\cos\theta_1^t,\cos\tilde{\theta}_1$ behavior of $\mathrm{Re}[\rho_{+-}]$ for $E_{\mathrm{c.m.}}=380$ GeV. The surface peaks at about $(-0.25, 0.25)$; the levels range from -0.5392 to 0.4179 with spacing 0.1063.

$$\cos\omega_1=\frac{E_{\mathrm{c.m.}}(m_t^2-m_W^2+[m_t^2+m_W^2]\beta\cos\theta_1^t)}{4m_t^2p_1}, \quad (75)$$

where $p_1=$the magnitude of the W^+ momentum in the $(tt)_{\mathrm{c.m.}}$ frame and γ and β describe the boost from the $(tt)_{\mathrm{c.m.}}$ frame to the t_1 rest frame [$\gamma=E_{\mathrm{c.m.}}/(2m_t)$ with $E_{\mathrm{c.m.}}=$ total energy of tt, in $(tt)_{\mathrm{c.m.}}$].

Note that the ρ_s term depends only on the W_L-W_T interference intensities, whereas the ρ_0 and ρ_c terms only depend on the polarized partial widths, specifically,

$$\rho_{0,c}=\frac{1}{2}[2-2\cos^2\omega_1\cos^2\tilde{\theta}_1-\sin^2\omega_1\sin^2\tilde{\theta}_1]\frac{\Gamma_L^{\pm}}{\Gamma}$$

$$\pm\frac{1}{4}[2+2\cos^2\omega_1\cos^2\tilde{\theta}_1+\sin^2\omega_1\sin^2\tilde{\theta}_1]\frac{\Gamma_T^{\pm}}{\Gamma}$$

$$\mp\cos\omega_1\cos\tilde{\theta}_1\frac{\Gamma_T^{\mp}}{\Gamma}, \quad (76)$$

with $\overline{\rho_{0,c}}=\rho_{0,c}$ $(1\to2$, add bars).

For the off-diagonal elements; the analogous expression is

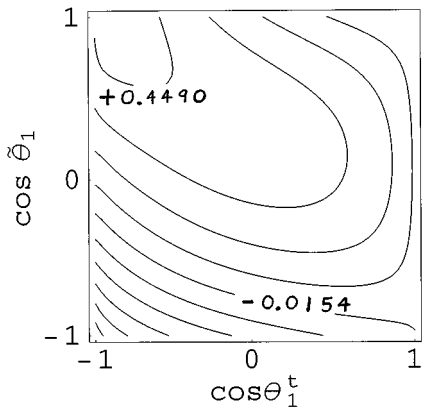

FIG. 12. The $\cos\theta_1^t,\cos\tilde{\theta}_1$ behavior of $\mathrm{Re}[\rho_{+-}]$ for $E_{\mathrm{c.m.}}=450$ GeV. The surface peaks at about $(-0.8, 0.9)$; the levels range from -0.5960 to 0.4490 with spacing 0.1161.

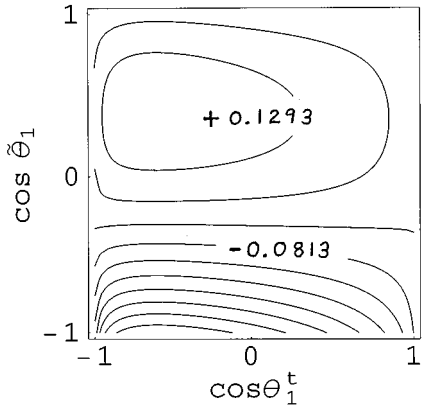

FIG. 13. The $\cos\theta_1^t,\cos\tilde{\theta}_1$ behavior of $\mathrm{Im}[\rho_{+-}]$ for $E_{\mathrm{c.m.}}=380$ GeV for arbitrary overall normalization $\omega'=\eta'=1$. The surface peaks at about $(-0.5, 0.5)$; the levels range from -0.5025 to 0.1293 with spacing 0.0702.

$$\rho_{+-}=\rho_c\sin\theta_1^t-\sqrt{2}(\eta\cos\theta_1^t-i\omega')\sin\omega_1\cos\tilde{\theta}_1,$$

$$+1/2\sqrt{2}(\omega\cos\theta_1^t-i\eta')\sin2\omega_1(2\cos^2\tilde{\theta}_1-\sin^2\tilde{\theta}_1). \quad (77)$$

Figures 7–14 show the $\cos\theta_1^t$, $\cos\tilde{\theta}_1$ behavior of the elements of these integrated or ''reduced'' composite density matrix $\rho_{hh'}$ assuming the $(V\text{-}A)$ values of Table I for the helicity parameters. These figures also show the dependence as the total center-of-mass energy $E_{\mathrm{c.m.}}$ of tt, in $(tt)_{\mathrm{c.m.}}$, is changed. Figure 7 is for ρ_{++} and $E_{\mathrm{c.m.}}=380$ GeV. The next one, Fig. 8, is for $E_{\mathrm{c.m.}}=450$ GeV. This dependence on $\cos\theta_1^t$, $\cos\tilde{\theta}_1$, i.e., the use of W decay-polarimetry, is the reason for the greater sensitivity of the S2SC function I_4 than the simpler energy-energy spin-correlation function $I(E_{W^+},E_{W^-})$; see Sec. VI. Figures 9 and 10 show the behavior of ρ_{--}. The behaviors of the real and imaginary parts of the off-diagonal elements ρ_{+-} are shown in Figs. 11–14. Note that to display the imaginary part with an arbitrarily fixed overall normalization, we have set $\omega'=\eta'$ in Eq. (77)

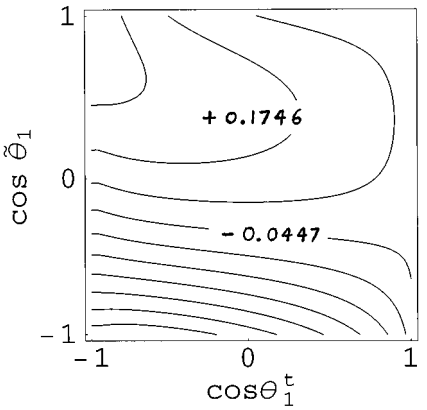

FIG. 14. The $\cos\theta_1^t,\cos\tilde{\theta}_1$ behavior of $\mathrm{Im}[\rho_{+-}]$ for $E_{\mathrm{c.m.}}=450$ GeV for arbitrary overall renormalization $\omega'=\eta'=1$. The surface peaks at about $(-1, 0.8)$; the levels range from -0.7025 to 0.2842 with spacing 0.1096.

since in the SM the relative phase $\beta_a^R=0$. If the (V-A) values for the helicity parameters are empirically found to be only approximately correct, then the details of the dependence of $\rho_{hh'}$ on $\cos\theta_1^t$,$\cos\widetilde{\theta}_1$, and $E_{\rm cm}$ will differ but, nevertheless, the analyzing power of $\rho_{hh'}$ and of **R** of Eq. (12) should remain large at both the Tevatron and the LHC.

D. Production density matrix elements

The production density matrix elements for $gg\to t\bar{t}$ are calculated by the methods in [15,12]. In the usual helicity phase conventions, we obtain

$$\rho_{++}(gg\to t\bar{t})=\rho_{++,++}=\rho_{--,--}$$
$$=\frac{m_t^2}{96E_t^2}\left[\frac{s^2}{(m_t^2-t)^2(m_t^2-u)^2}\right]\left[7+9\frac{p_t^2}{E_t^2}\cos^2\theta_t\right]$$
$$\times\left[1+\frac{p_t^2}{E_t^2}(1+\sin^4\theta_t)\right], \quad (78)$$

$$\rho_{+-}(gg\to t\bar{t})=\rho_{+-,+-}=\rho_{-+,-+}$$
$$=\frac{p_t^2}{96E_t^2}\left[\frac{s^2}{(m_t^2-t)^2(m_t^2-u)^2}\right]$$
$$\times\left[7+9\frac{p_t^2}{E_t^2}\cos^2\theta_t\right]\sin^2\theta_t(1+\cos^2\theta_t), \quad (79)$$

where E_t is the energy of the produced t quark with momentum of magnitude p_t at angle θ_t in the $(t\bar{t})_{\rm c.m.}$ frame.

The amplitudes for $q_i\bar{q}_i\to t\bar{t}$ in the helicity phase convention are easily obtained from those in Ref. [12]. The associated production density matrix elements are

$$\rho_{++}(q\bar{q}\to t\bar{t})=\rho_{++,++}=\rho_{--,--}=\frac{m_t^2}{9E_t^2}\sin^2\theta_t, \quad (80)$$

$$\rho_{+-}(q\bar{q}\to t\bar{t})=\rho_{+-,+-}=\rho_{-+,-+}=\tfrac{1}{9}(1+\cos^2\theta_t). \quad (81)$$

The normalization in these equations corresponds to the hard parton, differential cross sections

$$\frac{d\hat{\sigma}}{dt}=\frac{\alpha_s^2}{s^2}(\rho_{++,++}+\rho_{--,--}+\rho_{+-,+-}+\rho_{-+,-+}). \quad (82)$$

VI. ADDITIONAL REMARKS

The simpler stage-one spin-correlation function $I(E_{W^+},E_{W^-})$ of Ref. [5] directly follows from Eq. (69) by integrating out $\widetilde{\theta}_1$ and $\widetilde{\theta}_2$:

$$I(E_{W^+},E_{W^-})=\sum_i\{\rho_{+-}(q_i\bar{q}_i\to t\bar{t})^{\rm prod}[\rho_{++}\overline{\rho_{--}}+\rho_{--}\overline{\rho_{++}}]+\rho_{++}(gg\to t\bar{t})^{\rm prod}[\rho_{++}\overline{\rho_{++}}+\rho_{--}\overline{\rho_{--}}]\}, \quad (83)$$

where

$$\rho_{++}=1+\zeta\mathcal{S}_W\cos\theta_1^t, \quad \rho_{--}=1-\zeta\mathcal{S}_W\cos\theta_1^t,$$
$$\overline{\rho_{++}}=1-\zeta\mathcal{S}_W\cos\theta_2^t, \quad \overline{\rho_{--}}=1+\zeta\mathcal{S}_W\cos\theta_2^t. \quad (84)$$

However, using $I(E_{W^+},E_{W^-})$, the fractional sensitivity for measurement of ζ at the Tevatron at 2 TeV is only 38% versus 2.2% by using $I(E_{W^+},E_{W^-},\widetilde{\theta}_1,\widetilde{\theta}_2)$. The ''fractional sensitivity'' is explicitly defined by Eq. (36), in [6]. Similarly, at the LHC at 14 TeV, the fractional sensitivity for measurement of ζ with I_2 is 2.3% versus 0.39% with I_4. This shows the importance of including the analyzing power of the second stage in the decay sequence, i.e., W decay-polarimetry; cf. Sec. V C. It is also important to note that only the partial width and the ζ helicity parameter appear in this stage-one spin-correlation function. To measure the other helicity parameters $(\xi,\sigma,\ldots)$, one needs to use stage-two W or b decay-polarimetry, and/or other spin-correlation functions.

This use of W decay-polarimetery and I_4 to significantly increase the analyzing powers does not directly make use of the threshold-type kinematics at the Tevatron of the $q\bar{q}\to t\bar{t}$ reaction. See the series of papers by Parke, Mahlon, and Shadmi [7] for spin-correlation analyses which investigate threshold techniques.

Some modern Monte Carlo simulations do include spin-correlation effects, for instance, KORALB for e^-e^+ colliders [16]. The simple general structure and statistical sensitivities of the S2SC function I_4 show that spin-correlation effects should also be included in Monte Carlo simulations for $p\bar{p}$ or $pp\to t\bar{t}X\to\cdots$. In such a Monte Carlo simulation it should be simple and straightforward to build in the amplitudes for production of L-polarized and T-polarized $W^\pm$'s from distinct Lorentz-structure sources. Thereby, spin-correlation techniques and the results in this paper can be used for many systematic checks. For example, they could be used to experimentally test the CP and T invariance ''purity'' of detector components and of the data analysis by distinguishing which coefficients are or are not equal between various experimental data sets analyzed separately for the t and $\bar{t}$ modes.

Assuming only b_L couplings [17], a simple way for one to use a Monte Carlo simulation to test for possible CP violation is to add an $S+P$ coupling to the standard $V-A$ cou-

pling in the t decay mode such that the $S+P$ contribution has an overall complex coupling factor c in the t mode and a complex factor d in the $\bar{t}$ mode. This will generate a difference in moduli and phases between the t and $\bar{t}$ modes. Then the two tests for CP violation are whether $|c|=|d|$, $\arg(c)=\arg(d)$ experimentally.

To be model independent and of greater use to theorists, experimental analyses should not assume a mixture of only V and A current couplings in top-quark decays. By consideration of polarized partial widths, there are several fundamental quantities besides the chirality parameter and the total partial width which can be directly measured. For example, there are three logically independent tests for only b_L couplings: $\xi=1$, $\zeta=\sigma$, and $\omega=\eta$ up to $O(m_b)$ corrections [18]. If $\tilde{T}_{FS}$ violation were to occur, then the nonzero parameters $\omega'=\eta'$ if there are only b_L couplings.

ACKNOWLEDGMENTS

We thank experimental and theoretical physicists for discussions and assistance, in particular with respect to matters specific to hadron colliders. We thank Ming Yang, and for computer services, John Hagan, Christine Place-Sweet, and Mark Stephens. This work was partially supported by U.S. Department of Energy Contract No. DE-FG 02-96ER40291.

[1] CDF Collaboration, F. Abe *et al.*, Phys. Rev. Lett. **74**, 2626 (1995).

[2] D0 Collaboration, S. Abachi *et al.*, Phys. Rev. Lett. **74**, 2632 (1995).

[3] P. Tipton, *ICHEP'96*, Proceedings of the 28th International Conference on High Energy Physics, Warsaw, Poland, edited by Z. Ajduk and A. K. Wroblewski (World Scientific, Singapore, 1997), p. 123.

[4] M. Jacob and G. Wick, Ann. Phys. (N.Y.) **7**, 209 (1959); K.-C. Chou, Sov. Phys. JETP **36**, 909 (1959); M. I. Shirokov, *ibid.* **39**, 633 (1960); J. Werle, Phys. Lett. **4**, 127 (1963); S. M. Berman and M. Jacob, SLAC Report No. 43, 1965; Phys. Rev. **139**, B1023 (1965); R. D. Auvil and J. J. Brehm, *ibid.* **145**, 1152 (1966). Very readable treatments of the helicity formalism are in H. Pilkuhn, *Interaction to Hadrons* (North-Holland, Amsterdam, 1967); M. L. Perl, *High Energy Hadron Physics* (Wiley, New York, 1974); A. D. Martin and T. D. Spearman, *Elementary Particle Physics* (North-Holland, Amsterdam, 1970); M. L. Goldberger and K. M. Watson, *Collision Theory* (Wiley, New York, 1964); J. Werle, *Relativistic Theory of Reactions* (North-Holland, Amsterdam, 1966); J. D. Richman, Caltech Report No. CALT-68-1148 (unpublished); Caltech Report No. CALT-68-1231 (unpublished).

[5] C. A. Nelson, Phys. Rev. Lett. **41**, 2805 (1990); in *Results and Perspectives in Particle Physics*, edited by M. Greco (Editions Frontieres, Gif-sur-Yvette, France, 1994), p. 259.

[6] C. A. Nelson, B. T. Kress, M. Lopes, and T. P. McCauley, SUNY BING 5/27/97, hep-ph/9706469.

[7] V. Barger, J. Ohnemus, and R. J. N. Phillips, Int. Mod. Phys. A 4, 617 (1989); G. L. Kane, G. A. Landinsky, and C. P. Yuan, Phys. Rev. D **45**, 124 (1991); R. H. Dalitz and G. R. Goldstein, *ibid.* **45**, 1531 (1992); M. Jezabek and J. H. Kuhn, Phys. Lett. B **329**, 317 (1994); G. A. Landinsky and C. P. Yuan, Phys. Rev. D **49**, 4415 (1994); E. Malkawi and C. P. Yuan, *ibid.* **50**, 4462 (1994); G. Mahlon and S. Parke, *ibid.* **53**, 4886 (1996); hep-ph/9706304; S. Parke and Y. Shadmi, Phys. Lett. B **387**, 199 (1996); T. Stelzer and S. Willenbrock, *ibid.* **374**, 169 (1996); A. Brandenburg, *ibid.* **388**, 626 (1996); B. Grzadkowski and Z. Hioki, *ibid.* **391**, 172 (1997); in *High Energy Spin Physics*, Proceedings of the Workshop, Kobe, Japan, 1996, edited by T. Morii and S. Mukherjee (Kobe University, Kobe, 1997), hep-ph/9610306; D. Chang, S.-C. Lee, and A. Sumarokov, Phys. Rev. Lett. **77**, 1218 (1996); A. P. Heinson, A. S. Belyaev, and E. E. Boos, hep-ph/9612323; K. Cheung, Phys. Rev. D **55**, 4430 (1997).

[8] J. F. Donoghue and G. Valencia, Phys. Rev. Lett. **58**, 451 (1987); C. A. Nelson, Phys. Rev. D **30**, 1937 (1984); J. R. Dell'Aquila and C. A. Nelson, *ibid.* **33**, 80 (1986); **33**, 101 (1986); W. Bernreuther, J. P. Ma, T. Schroder, and T. N. Pham, Phys. Lett. B **279**, 389 (1992); W. Bernreuther, O. Nachtmann, P. Overmann, and T. Schroder, Nucl. Phys. **B388**, 53 (1992); C. R. Schmidt and M. E. Peskin, Phys. Rev. Lett. **69**, 410 (1992); D. Chang and W.-Y. Keung, Phys. Lett. B **305**, 261 (1993).

[9] J. P. Ma and A. Brandenburg, Z. Phys. C **56**, 97 (1992); T. Arnes and L. M. Sehgal, Phys. Lett. B **302**, 501 (1993); D. Atwood, G. Eilam, A. Soni, R. Mendel, and R. Migneron, Phys. Rev. Lett. **70**, 1364 (1993); R. Crux, B. Grzadkowski, and J. F. Gunion, Phys. Lett. B **289**, 440 (1992); B. Grzadkowski, B. Lampe, and K. J. Abraham, hep-ph/9706489.

[10] C. A. Nelson, Phys. Rev. D **53**, 5001 (1996); Phys. Lett. B **355**, 561 (1995).

[11] C. A. Nelson, H. S. Friedman, S. Goozovat, J. A. Klein, L. R. Kneller, W. J. Perry, and S. A. Ustin, Phys. Rev. D **50**, 4544 (1994).

[12] C. A. Nelson, Phys. Rev. D **43**, 1465 (1991).

[13] C. A. Nelson, Phys. Rev. D **30**, 1937 (1984); J. R. Dell'Aquila and C. A. Nelson, *ibid.* **33**, 101 (1986).

[14] CDF Collaboration, F. Abe *et al.*, Phys. Rev. Lett. **79**, 1992 (1997); P. Giromini, presented at the International Lepton-Photon Symposium, Hamburg, Germany, 1997.

[15] M. Gluck, J. F. Owens, and E. Reya, Phys. Rev. D **17**, 2324 (1978); H. Georgi, S. L. Glashow, M. E. Machacek, and D. V. Nanopoulos, Ann. Phys. (N.Y.) **114**, 273 (1978).

[16] S. Jadach and Z. Was, Comput. Phys. Commun. **36**, 191 (1985); **64**, 275 (1991); **85**, 453 (1995).

[17] Historically, for a complete Lorentz-invariant characterization of the charged current, there have been two popular choices for the minimal sets of couplings: Express the vector matrix element $\langle b|v^\mu(0)|t\rangle$ either in terms of V, f_M, and S^- (recall S^- does not contribute to the on-shell W^+ mode) or of V, S, and S^-. Correspondingly, express the axial $\langle b|a^\mu(0)|t\rangle$ either in terms of A, f_E, and P^- (P^- does not contribute to the on-shell W^+ mode) or of A, P, and P^-. So if there are only b_L couplings, then the chiral combinations of $V-A$ and $S+P$ can contribute significantly to the W^+ mode since m_b/m_t, $m_b/m_w \cong 0$. To include b_R couplings, one would add $V+A$ and

$S-P$ via an additional ''$g_R\gamma^\mu(1+\gamma_5)+e(k+p)^\mu(1-\gamma_5)$'' for t and ''$\overline{g_R}\gamma^\mu(1+\gamma_5)+f(k+p)^\mu(1-\gamma_5)$'' for $\bar{t}$ where e and f are different complex coupling factors. In each case this gives the expected number of independent variables. Measurement of the overall relative phase of the $\lambda_b=-\frac{1}{2}$ and $\lambda_b=\frac{1}{2}$ couplings (and for the $\lambda_b=\pm\frac{1}{2}$ couplings of the anti-b quark) by S2SC's using b quark-polarimetry is considered in Ref. [6].

[18] The corrections for $m_b=4.5$ GeV are given numerically in Table 3 of Ref. [6] and follow analytically from Eqs. (25)–(28) in the present paper.